PHOTODISSOCIATIVE GENERATION OF A POPULATION INVERSION FOR THE THALLIUM-MERCURY EXCIMER SYSTEM

by

Mark Joseph Retter

A Thesis Submitted to the Faculty of the

DEPARTMENT OF ELECTRICAL AND COMPUTER ENGINEERING

In Partial Fulfillment of the Requirements
For the Degree of

MASTER OF SCIENCE
WITH A MAJOR IN ELECTRICAL ENGINEERING

In the Graduate College

THE UNIVERSITY OF ARIZONA

1 9 8 5

STATEMENT BY AUTHOR

This thesis has been submitted in partial fulfillment of requirements for an advanced degree at The University of Arizona and is deposited in the University Library to be made available to borrowers under rules of the Library.

Brief quotations from this thesis are allowable without special permission, provided that accurate acknowledgment of source is made. Requests for permission for extended quotation from or reproduction of this manuscript in whole or in part may be granted by the head of the major department or the Dean of the Graduate College when in his or her judgment the proposed use of the material is in the interests of scholarship. In all other instances, however, permission must be obtained from the author.

SIGNED: Mark J Retter

APPROVAL BY THESIS DIRECTOR

This thesis has been approved on the date shown below:

Roger C. Jones
Professor of Electrical and
Computer Engineering

September 24, 1985
Date

ACKNOWLEDGMENTS

I wish to thank Professor Roger C. Jones for his guidance and technical advice. Thanks must be given also to Professor Olgierd A. Palusinski and Ian Scott-Fleming for their help on computer problems. Finally, I wish to thank the staff of the Department of Electrical and Computer Engineering and Sally Adams for their assistance in making the job of typing this thesis so much easier.

TABLE OF CONTENTS

TABLE OF CONTENTS--Continued

LIST OF ILLUSTRATIONS

LIST OF TABLES

ABSTRACT

Recent advances in technology have led to the development of efficient, high energy, ultraviolet excimer lasers, which were theoretically investigated in the early 1960's. Studies have shown that some metal vapor gas systems have great potential to be implemented as a medium for excimer lasing action.

Experimental evidence indicates that the thallium-mercury metal vapor system is one of the best candidates in this group. Arc discharge and e-beam excitation of this system generated a population inversion of thallium-mercury excimers necessary to cause superfluorescent emission, but the technological requirements limit the practical implementation of this system as a laser.

This thesis examines a thallium iodide-mercury gas mixture, in which photodissociation of thallium iodide is used to produce the excited thallium atoms necessary for the formation of thallium-mercury excimers. A model for short pulse optical excitation of the gas mixture, using this pumping method, is derived and used to examine the generation of an inversion for the excimer system. Recommendations for future experimental work are given for the proposed system so that a practical thallium-mercury excimer laser may be built.

CHAPTER 1

INTRODUCTION

Molecular gas lasers, CO_2 and dye lasers, for example have been in existence for many years. However, the output of such lasers were usually a result of either vibrational, rotational or vibrational-rotational transitions in molecules of the laser media. The concept of using electronic transitions in molecules known as excimers was proposed by Houtermans (1960), but successful demonstrations in the laboratory did not occur until the early 1970's. Since then many excimer systems have been examined, and today one can purchase benchtop excimer laser systems that can achieve one joule per pulse output, with an energy efficiency in the 0.1 to 2.0% range.

An excimer, a molecule in an excited state, can be looked at in the following manner: If both atoms are in their respective ground states, the atoms would usually be repulsive. But, if one atom is in an excited electronic state, this atom may form a strong bond with the ground state atom, creating a bound excited state called an excimer. Two ground state atoms may form a bound molecular state, and excimers can be formed by open shell fragments, but I will consider only the previously mentioned case. There can be many excimer states for a molecular system, and the total set of energy states can be quite complicated (Fitzsimmons 1973, p. 477).

The excimer system I will investigate, thallium mercury, denoted ($TLHG^*$), is created by an excited thallium atom (TL^*) in the TL $7^2S1/2$ state, forming a bond with a ground state mercury atom (HG). When $TLHG^*$ de-excites, releasing an optical photon, it stays together as a molecule in what is known as a bound repulsive state. Within a vibrational lifetime of the molecule, the molecule dissociates into its parent atoms in their respective ground states.

One can already see a prime advantage of an excimer system. The fact that the molecule quickly dissociates once it is in its ground state essentially says that there is no ground state. Therefore a population inversion, essential for stimulated emission to dominate, is generated by the mere production of $TLHG^*$! This entails the production of TL^* and the formation of $TLHG^*$ from TL^* and HG. This leads to the primary focus of this paper, which is to consider a method of producing TL^* and the resultant generation of a population inversion in the TLHG excimer system.

Photodissociation of salts have proved highly efficient in yielding large quantities of excited atomic species (Maya 1979, pp. 579-86). In several experiments thallium iodide (TLI) was photodissociated by UV radiation for the purpose of producing TL^*. An overall efficiency of 50% was achieved in producing a TL $7^2S1/2$ atom per molecule dissociated. This high efficiency in yielding the metastable Tl $7^2S1/2$ atom led to the creation of the thallium photodissociation laser, which has an energy efficiency of 14% (Maya 1979, pp. 579-86). Using a simple model, and the experimental results of others, Shahdin,

Ludewigt and Wellegehausen (1981, pp. 1276-80) showed that photodissociating cesium iodide (CSI) in the presence of xenon ground state atoms (XE) yielded the CSXE excimer in sufficient quantity to generate the population inversion necessary for lasing to occur. They later used this technique in the laboratory to produce the TLHG excimer from TLI and HG (Ludewigt et al. 1982, pp. 143-47). I will examine, using the model of Shahdin et al. (1981, p. 1279) and the experimental results of others, the feasibility of using the previously mentioned pumping scheme to generate a threshold population inversion in the TLHG excimer system.

Chapter 2 examines in some detail the mechanics of excimer systems and the TLHG excimer system. A brief review of the basic laser equations and comparison of the TLHG excimer system to the TLXE excimer system is included.

In Chapter 3 general information about TL, TLI, and HG is is discussed, including the details of photodissociating TLI and the reformation of TLI from its parent atoms. An examination of some of the engineering problems encountered will ensue.

Chapter 4 ties together the previous chapters in sufficient detail to enable proposing and justifying the model to be employed. A look into the experimental results of other investigations is used as additive support of the model chosen. The analysis and interpretation of the quantitative results predicted by the model is performed, using a variation of several parameters.

Chapter 5 presents conclusions and recommendations for implementing the proposed pumping scheme for the TLHG excimer system.

CHAPTER 2

THE THALLIUM-MERCURY EXCIMER SYSTEM

The following sections describe various aspects of excimers in general and the specifics of the TLHG excimer. A comparison to the TLXE excimer system is used to point out the desired qualities of the TLHG excimer.

Excimers in General

I have already described how specific kinds of excimer states are formed. At present, many of these excimer states are not well understood, but we can describe the states in terms of extreme categories. The ground state of a diatomic excimer system can either be "repulsive" or "flat". A repulsive ground state arises from a decreasing potential, V(R), as a function of the distance between the atoms, R. The flat ground state arises from a relatively constant potential, which has little functional dependence on R. Repulsive curves for the potential also occur from a charge overlap between atomic orbitals. An example of this is the p orbital of an alkali atom interacting with the closed shell of a rare gas atom. An electron in the $p\sigma$ orbital of the alkali atom together with the rare gas atom produces a repulsive potential, whereas a $p\pi$ orbital electron interacting with the rare gas atom produces a relatively flat potential. Flat potentials are also produced from ground state mixing with bound

excited configurations and produce some bound character; however, this is true for only weak mixing of these states (Rhodes 1984, p. 6). See Figure 1 for a comparison of these states, along with a stable ground state of a diatomic molecule.

The bonding characteristics of excited states results from a combination of three physical conditions: covalent bonding, charge transfer, and rydberg states. An excimer state is formed by covalent bonding when the parent atoms share electron(s). Group II homonuclear molecules (HG_2 or MG_2) are an example of molecules formed by this mechanism. The charge transfer state results from ionic bonding of two atoms of equal but opposite charges in the case of diatomic systems. The rydberg state can be best described briefly from the orbital characteristics of the atoms involved. Here orbitals are relatively diffuse with little bonding characteristics. In short, one must examine the limiting positive ion curve of the particular state in question (Rhodes 1984, p. 7). The mixing of rydberg and charge transfer states can be significant and complicates the the total excimer energy state. The mixing of charge transfer and covalent states can help determine energy curves of both ground and excited states, as is the case for the TLI ground state.

The Basic Equations

The complicated energy state of an excimer system makes it difficult to investigate the system solely on a theoretical basis. Using experimentally determined information and semiclassical laser theory, one can calculate desired quantities necessary to describe the

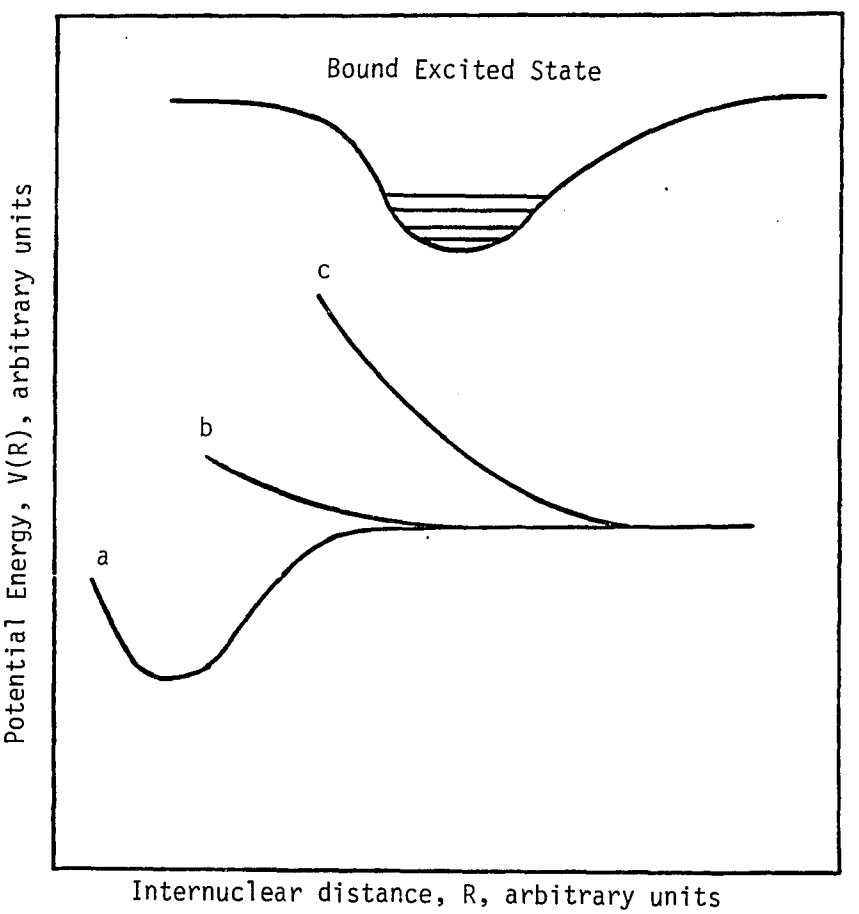

Figure 1. Examples of molecular energy states; a) stable ground state, b) flat ground state, c) repulsive ground state.

excimer system. An evaluation of the system then can be made to determine if the system is a potential laser candidate. The following is an edited derivation of the relevant equations, as described by A. Gallagher in "Excimer Lasers" (Rhodes 1984, pp. 139-48).

To begin, let us look at the relation resulting from Einstein's treatment of induced and spontaneous transitions at wavelength λ and frequency ν, between atomic electronic states.

$$B_{21} = \frac{\lambda^2}{8\pi} \cdot \frac{c}{h\nu} \cdot A_{21} \tag{2.1}$$

We define state 2 as the upper state and state 1 as the lower state of the transition, where B_{21} is the stimulated emission rate with dimensions of $cm^3/(watt\text{-}sec^3)$, and A_{21} is the spontaneous emission coefficient with dimensions of sec^{-1}. Multiplying both sides of equation (2.1) by $(h\nu/c)N_2$, where N_2 is the upper state population number density in cm^{-3}, leads us to the following relation:

$$\frac{h\nu}{c} N_2 B_{21} = \frac{\lambda^2}{8\pi} N_2 A_{21} \tag{2.2}$$

We must first generalize equation (2.2) to consider a continuum of states, which is the case for molecular electronic transitions. We first replace $N_2 A_{21}$ with a spectral distribution, $\delta(\nu)\, d\nu$, which describes the number of spontaneously emitted photons from state 2 at frequency ν for the frequency interval $d\nu$ per unit volume. The left-hand side of equation (2.2) represents the gain per unit length for the frequency interval $d\nu$ for stimulated emission from state 2 at

frequency ν, which is defined as $G(\nu)\, d\nu$. Making the above substitutions into equation (2.2), we now have the following:

$$G(\nu)\, d\nu = \frac{\lambda^2}{8\pi}\, \delta(\nu)\, d\nu \tag{2.3}$$

If we wish to examine the entire line for the molecular electronic radiative transition, we integrate equation (2.3) with respect to ν, where λ is the wavelength at the center of the band and is considered a constant. Gallagher and others maintain this mixed format of wavelength and frequency in their derivations, but for the purpose of clarity the final equation will be converted to a frequency dependent relation.

The usual absorption coefficient $k(\nu)$, is defined as the difference between pure absorption, $K(\nu)$, and $G(\nu)$; $k(\nu) = K(\nu) - G(\nu)$. If we consider a container with a vapor in equilibrium at temperature T, net absorption at each ν must be balanced by spontaneous emission at the same ν. This can properly be described, if we consider atomic electronic transitions, by:

$$N_{21}A_{21} = B_{12}N_1\, \rho(\nu) - B_{21}N_2\, \rho(\nu) \tag{2.4}$$

where $\rho(\nu)$ is the radiation density for a blackbody in thermal equilibrium:

$$\rho(\nu) = \frac{8\pi}{\lambda^2}\frac{h\nu}{c}\left[\exp\left(\frac{h\nu}{kT}\right)-1\right]^{-1} \tag{2.5}$$

Substituting and rearranging terms produces the following relation:

$$\frac{\lambda^2}{8\pi} N_2 A_{21} = \{\exp(\frac{h\nu}{kT})-1\}^{-1}\{\frac{h\nu}{c} N_1 B_{12} - \frac{h\nu}{c} N_2 B_{21}\} \qquad (2.6)$$

Recalling our previous definitions in considering molecular electronic transitions this equation becomes:

$$\frac{\lambda^2}{8\pi} \delta(\nu) = k(\nu)[\exp(\frac{h\nu}{kT})-1]^{-1} \qquad (2.7)$$

where we have dropped $d\nu$ from both sides of equation (2.7). Substituting in for $k(\nu)$, $K(\nu) - G(\nu)$, and rearranging, produces:

$$\delta(\nu) = \{K(\nu) - G(\nu)\}\{\frac{8\pi}{\lambda^2} (\exp(\frac{h}{kT})-1)^{-1}\} \qquad (2.8)$$

Substituting in for $\delta(\nu)$ using equation (2.3), gives us a relationship between $K(\nu)$ and $G(\nu)$:

$$\frac{G(\nu)}{K(\nu)} = \exp[\frac{h\nu}{kT}] \qquad (2.9)$$

For an atomic system in equilibrium, on the other hand, the ground and excited state states are related by:

$$\frac{[C^*]}{[C]} = \frac{g^*}{g} \exp(\frac{-h\nu_o}{kT}) \qquad (2.10)$$

where $[C^*]$ is the excited state density with a degeneracy of g^* and $[C]$ is the ground state density of the atoms, with a degeneracy of g. Equations (2.9) and (2.10) describe the equilibrium conditions for the molecular system and the parent atomic system, respectively. In combining these the two equations, the result is a relationship between

the number density of the excited parent atoms and the ratio of the gain and absorption coefficients for the excimer states of the molecular system:

$$\frac{G(\nu)}{K(\nu)} = \frac{[C^*]}{[C]} \cdot \frac{g}{g^*} \cdot \exp\left[\frac{-h(\nu-\nu_o)}{kT}\right] \tag{2.11}$$

The classical Franck-Condon principle predicts that the distance between atoms, R, in a molecule, remains constant during an electronic radiative transition. Let us define $V_i^*(R)$ as the electronic energy of the i^{th} adiabatic state of an excimer, CB^*, (which dissociates into C^* + B) and $V_j(R)$ as the electronic energy of the j^{th} adiabatic state of CB (which dissociates into C + B). If B, after dissociation is in a $^1S_0$ state with statistical weight gb=1, then C^* + B forms gc^* adiabatic states and C + B forms gc adiabatic states. Now, the total spontaneous emission rate per unit volume, $\delta(\nu)\, d\nu$, is given by the product of the total number density of the excimers with internuclear separations between between R and R + dR, that emit photons of frequency ν within the band $d\nu$ (predicted by the Franck-Condon principle) and the spontaneous emission rate coefficient from state i to state j, $A(R)_{ij}$, for all radiative transitions where $h\nu = V^*(R) - V(R)$. Recalling our previous relation for $\delta(\nu)$, we arrive at the following:

$$\delta(\nu)\, d\nu = \sum_{ij} A(R)_{ij}\, d[CB^*]_i \tag{2.12}$$

where $d[CB^*]_i$ is the number density of the excimer in the i^{th} adiabatic state with internuclear seperation between R and R + dR. Using

equation (2.3) we come up with the following relationships for $G(\nu)$ and $K(\nu)$:

$$G(\nu) = \frac{\lambda^2}{8\pi} \sum_{ij} A(R)_{ij} \frac{d[CB^*]_i}{d\nu} \tag{2.13}$$

$$K(\nu) = \frac{\lambda^2}{8\pi} \sum_{ij} \frac{g_i^*}{g_j} A(R)_{ij} \frac{d[CB^*]}{d\nu} \tag{2.14}$$

If we take the average of $A(R)_{ij}$ and let $d\nu$ go to $\Delta\nu$ for the band, the result is the familiar expression used for $G(\nu)$:

$$\frac{G(\nu)}{[CB^*]_i} = \frac{\lambda^2}{8\pi} \cdot \frac{\overline{A_i}}{\Delta\nu} \tag{2.15}$$

We then convert λ to ν_o, the center frequency for the band, and equation (2.15) becomes the following:

$$\frac{G(\nu)}{[CB^*]_i} = \frac{c^2}{\nu_o^2 8\pi} \cdot \frac{\overline{A_i}}{\Delta\nu} \tag{2.16}$$

Frequently, $\overline{A_i}$ goes to A_o, the spontaneous rate coefficient of the excited parent atomic system.

The derivations described are sufficient to examine, in some detail, the results for the TLHG excimer system. A more rigorous derivation by Hedges, Drummond and Gallagher (1972) and Phelps (1972) yields the following expressions for $G(\nu)$:

$$G(\nu) = \frac{\lambda^2}{8\pi} \sum_{ij} A(R)_{ij} \left(\frac{d^3R}{d\nu}\right) \frac{g_i^*}{g_c^*} [C^*][B] \exp\left\{\frac{[-V_i^*(R) - V_i(\infty)]}{kT}\right\} \tag{2.17}$$

The important point to note is the temperature and potential well depth dependence of $G(\nu)$.

Desired Quantities in an Excimer System

The major kinetic processes of interest in an excimer laser system can be seen in Figure 2. First, we excite a ground state atom into an upper state. This can be done using many pumping schemes, and each process has its advantages and disadvantages, to be discussed later. In this metastable excited state, the atom combines with a ground state atom of the same or different species to form an excimer. As shown in Figure 2, as will be the case for $TLHG^*$, this process occurs by three body association. If the excimer is in a high vibrational state, it must de-excite into lower vibrational levels before stimulated emission can occur. Once the excimer undergoes an electronic radiative transition to the repulsive ground state, it dissociates into its parent atoms in their respective ground states, and the entire process can be repeated.

The rate at which these processes occur depends on the shape of the potential curves which describe the system. The formation rate of the excimer depends on the square of the ground state atomic density of the non-excited atom and the "width" of the potential well associated with the excimer state. The wider the well, in terms of the internuclear distance between the atoms, the larger the cross section is for the excimer formation to occur. This leads to a large formation rate constant. The depth of the potential well determines two important factors: the dissociation rate constant for the excimer state and the number of vibrational levels of the excimer state. The more shallow the well, the easier it is to dissociate the excimer. This imposes a

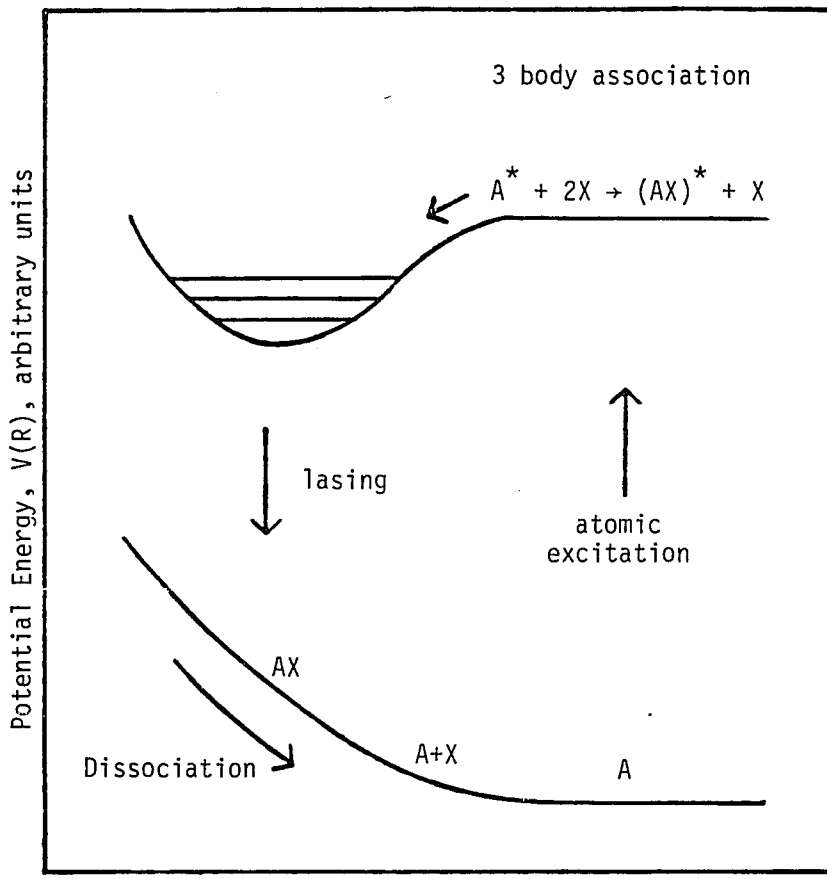

Figure 2. Energy and kinetic model of a typical excimer laser system

limitation on the temperature of the system, because the thermal energy of the excimer may be sufficient to cause dissociation. Collisional dissociation also plays a major role in excimer losses, and for TLHG, the bulk of this results from $TLHG^* + HG \rightarrow TL\ 7^2S1/2 + 2HG$. The advantage of a shallow well is that the majority of electrons will be available for lasing, because there are less high lying vibrational states for the electrons to populate. The result of these phenomena forces us to accept compromises in choosing an excimer system, with either a wide shallow potential well or a deeper, more narrow potential well.

The repulsive ground state allows the dissociation of the molecule into its parent atoms to occur rapidly, so the entire process can be repeated. The steeper the repulsive curve, the more rapid the dissociation occurs, usually within a vibrational lifetime of the molecule. This mechanism helps to maintain the population inversion generated by preventing the build up of ground state molecules. However, a repulsive potential curve that is too steep provides a larger spread of energy for the electronic radiative transition. This translates to a larger bandwith for the line, which results (see equation 2.17) in a lower value for the gain coefficient $G(\nu)$.

$TLHG^*$ Versus $TLXE^*$

The thallium xenon excimer ($TLXE^*$) has been studied extensively. At present, a laser based on the $TLXE^*$ system has not been demonstrated, but the results of experiments suggest that it is a promising laser candidate. The $TLHG^*$ system has been examined in some

detail also, and preliminary investigations show that it has greater potential, as a laser candidate, than $TLXE^*$. See Figures 3 and 4 for energy level diagrams of these systems.

The similarity of these systems enables us to make some comparisons between the two, so we can see the advantages and disadvantages of each system. In both systems, the excimer is formed by three body association involving the TL $7^2S1/2$ atom and two ground state atoms of the other species. The reaction can be described by TL $7^2S1/2$ + 2X -> TLX^* + X. The three body association rate constants of these two systems are similar in magnitude, the difference being a result of a different $V^*(R)$ for each system. $TLXE^*$ has a minimum potential at an internuclear radius of 3.1 angstroms with a well depth of 0.161 eV. $TLHG^*$ has a potential minimum at 3.1 angstroms with a well depth of 0.508 eV. In looking at equation (2.17), we can see that at a temperature of 700 degrees Kelvin the gain for $TLXE^*$ has an exponential factor of 2.81, whereas for $TLHG^*$, the gain has an exponential factor of 8.88. All others things considered roughly equal, this leads to a gain coefficient for $TLHG^*$ which is well over 100 times larger than that of $TLXE^*$. The width of the $TLXE^*$ potential well is 2 angstroms versus 1 angstrom for $TLHG^*$. As we expect, then, the association rate constant for $TLXE^*$, 5.0×10^{-31} cm^6/sec, is slightly larger than that of $TLHG^*$, 3.0×10^{-31} cm^6/sec.

A final major difference can be seen in examining the lower repulsive states of the systems. When $TLXE^*$ goes through an electronic radiative transition to either of its lower states, a larger bandwidth

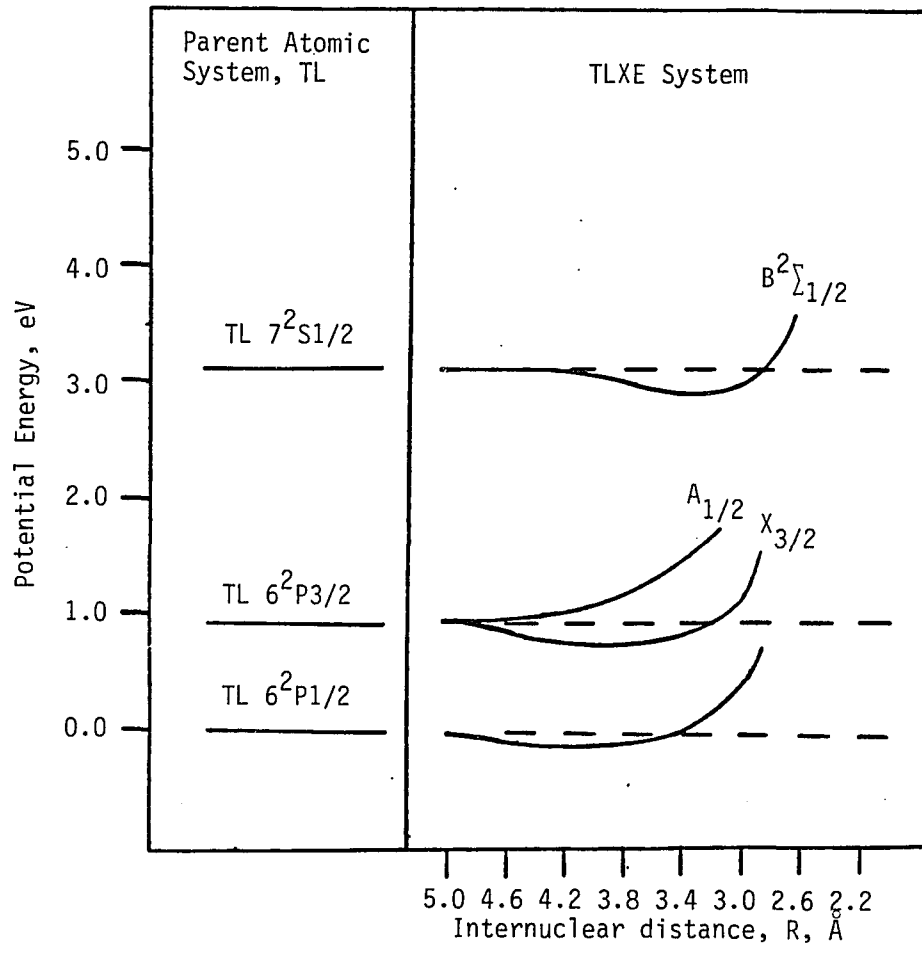

Figure 3. Energy level diagram for the TLXE excimer system

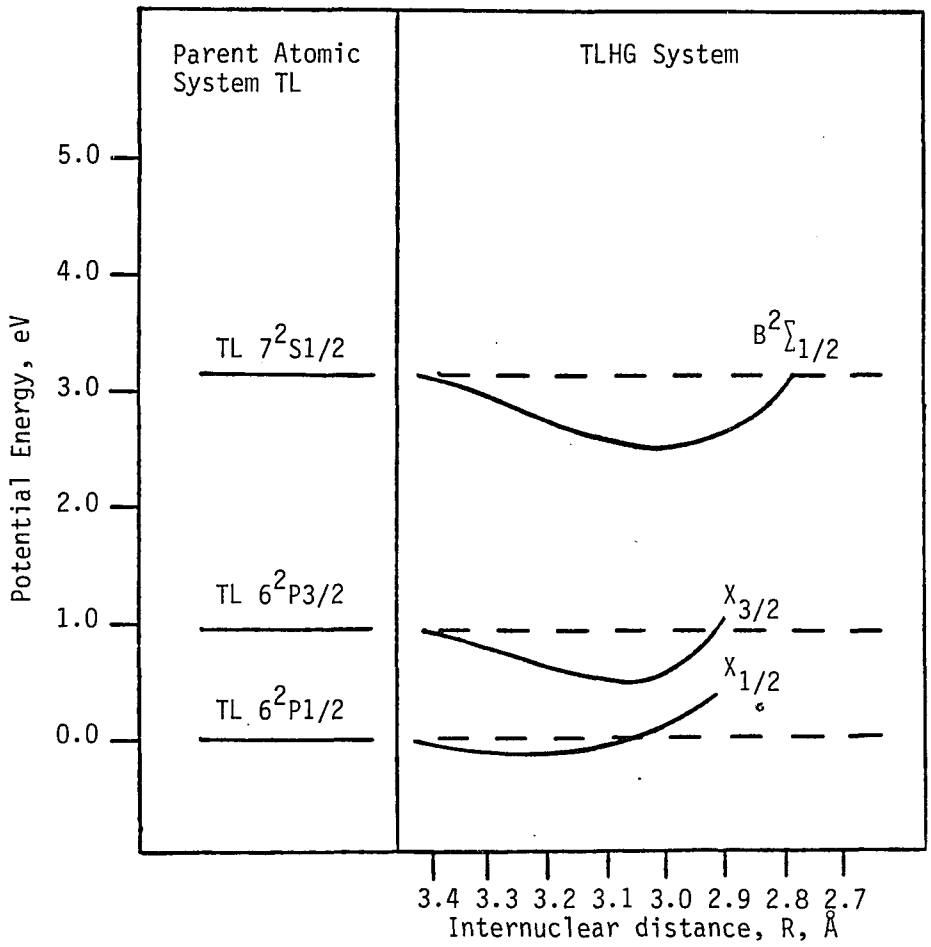

Figure 4. Energy level diagram for the TLHG excimer system

for the transition occurs because $V^*(R) - V(R)$ increases rapidly. The gain for the line is therefore reduced due to the larger value of $\Delta\nu$, which is shown by equation (2.17). $TLHG^*$, on the other hand, goes through electronic radiative transitions where $V^*(R) - V(R)$ is at a minimum. This allows more excimers to radiate at roughly the same wavelength, and the result leads to a more narrow spectral linewidth, which leads to a higher gain coefficient.

CHAPTER 3

THE THERMAL GAS MIXTURE AND PHOTODISSOCIATION OF THALLIUM IODIDE

Various pumping schemes have been used to generate a population inversion for TLHG*. The technological requirements in building the total system depends on the pumping scheme employed. The following sections attempt to show the reasons for using the photodissociation of TLI for the generation of a population inversion for TLHG*, as well as the advantages of using this pumping scheme over others that have been used.

General Information on Thallium

Thallium, as we know, is a group IIIA metal with one valence electron and a first ionization potential of 6.106 eV. For other facts about TL, refer to Table 1 (Chemical Rubber Company 1975, D-174). The melting point of TL, 305.5°C, is low enough so that one can deal with liquid TL on a practical engineering basis, but the boiling point, 1457 $\pm$ 10°C, is far too high to allow TL in the pure vapor state to be used in a gas laser system. This is the case for most metals used in laser systems, and, as a result, one must consider only the vapor pressure of these metals, noting if metal atoms are available in sufficient quantity to produce the threshold inversion necessary for lasing action to occur. The number densities of TL for the corresponding temperatures are listed in Table 2. They were determined by converting vapor

Table 1. Physical properties of thallium

Description of the constant	Value
Atomic number	81
Atomic weight	204.37 grams/mole
Melting point	305.5°C
Boiling point	1457±10°C
Van der Waal's a coefficient	--
Van der Waal's b coefficient	--
Ground state	$6^2P1/2$
First metastable state	$6^2P3/2$
Second metastable state	$7^2S1/2$
Lifetime of 1st metastable state	0.2325 sec
Lifetime of 2nd metastable state	7.5 nsecs

Table 2. Vapor pressure of thallium, thallium iodide and mercury

Temperature °C	Thallium #/cm^3	Thallium Iodide #/cm^3	Mercury #/cm^3
340.0	4.29×10^{9}	4.69×10^{14}	8.75×10^{18}
350.0	7.23×10^{9}	6.93×10^{14}	1.04×10^{19}
360.0	1.20×10^{10}	1.01×10^{15}	1.22×10^{19}
370.0	1.95×10^{10}	1.45×10^{15}	1.44×10^{19}
380.0	3.14×10^{10}	2.07×10^{15}	1.67×10^{19}
390.0	4.97×10^{10}	2.93×10^{15}	1.94×10^{19}
400.0	7.76×10^{10}	4.07×10^{15}	2.25×10^{19}
410.0	1.20×10^{11}	5.62×10^{15}	2.58×10^{19}
420.0	1.82×10^{11}	7.69×10^{15}	2.96×10^{19}
430.0	7.31×10^{11}	1.04×10^{16}	3.37×10^{19}
440.0	1.07×10^{12}	1.39×10^{16}	3.57×10^{19}

pressure data (Nesmeyanov 1963, p. 241) into number densities by the use of Van der Waal's equation:

$$\left(P - \frac{n^2 a}{V}\right)\left(V - nb\right) = nRT \qquad (3.1)$$

where P is the pressure in atmospheres, V is the volume in liters, n is the number of moles, R is the universal gas constant, 8.02568×10^{-2} liters-atom per mole-Kelvin, T is the temperature in Kelvin, a is the Van der Waal's a coefficient in liters^2-atm per mole^2, and b is the Van der Waal's b coefficient in liters per mole. Unfortunately, no information was available on the Van der Waal's coefficients for TL; therefore, I treated TL vapor as an ideal gas, where a = b = 0. The result converts equation (3.1) into the familiar expression which relates P, V and T for an ideal gas:

$$PV = nRT \qquad (3.2)$$

Furthermore, in checking the results with number densities quoted in other sources (Schlie et al. 1980, p. 4530), treating TL vapor as an ideal gas appears to be a valid assumption. In looking at Table 2, we see that at 440°C TL vapor achieves a number density of 1.07×10^{12} cm^{-3}. The required number density for TL or TLI needs to be greater than 10^{14} cm^{-3} for the proposed system. For TL, this requires a system temperature of over 800°C, and this is one of the reasons for using TLI instead of TL, as will be discussed later.

Hamil et al. (1979, p. 637) and Drummond and Schlie (1976, p. 3454) did use TL instead of TLI in their metal vapor system, but the

required temperature caused some engineering difficulties. Using discharge pumping or e-beam pumping, they produced TL $7^2S1/2$ atoms in sufficient quantity to generate a population inversion in the TLHG* system. Superfluorescent emission was observed, but no lasing action occurred. The difficulty in using these methods is threefold; the high temperature, besides causing engineering problems, reduces the gain (see equation 2.17) for the system and adds additional energy to the gas mixture, which in turn increases the losses due to collisional effects. The increased energy also decreases the formation rates of the excimers, in that the atoms must be "cooled" before they can combine to form the excimers in low lying vibrational states.

Regardless of whether TL or TLI is used, one major loss, in producing TLHG* is stimulated emission, due to radiative transitions from the TL $7^2S1/2$ state to the TL $6^2P3/2$ and the TL $6^2P1/2$ states. The metastable lifetime of the TL $7^2S1/2$ state is 7.5 nsecs (Gallagher and Lurio 1964, pp. 87-105). The ratio of of the intensities for these two transitions from the TL $7^2S1/2$ state is approximately 1. The thallium photodissociation laser based on these two lines was investigated by Ehrlich, Osgood and Maya (1978, pp. 579-93), and the results were quite promising. Unfortunately, for our system, this is a major loss which causes an additional problem, the production of the TL $6^2P3/2$ state, which has a very long metastable lifetime, 0.235 secs. This long lifetime creates a quenching problem, because the reformation of TLI requires TL $6^2P1/2$ atoms.

General Information on Mercury

Mercury is a group IIA atom with a full 6S subshell and a first ionization potential of 10.434 eV. Other facts about HG are given in Table 3. It turns out that HG can be excited from its ground state to create the HG_2^* system (see Figure 5), which was investigated by Carbone and Litvak (1968 p. 2413). For the model proposed, we will not consider formation of HG excimers or excited HG states, but we will investigate the use of these to examine some proposed pumping schemes which produce TLHG* in an indirect way. The boiling point of HG is 356.58°C (Chemical Rubber Company 1975, p. D-174), and because the temperature of the system will be higher than this, we will be able to control the density of the HG atoms by varying the initial HG total mass. Mercury in its vapor state can not be considered an ideal gas. The number densities listed in Table 2 were calculated using equation (3.1) and the vapor pressure data from Nesmeyanov (1963, p. 241). Checking these numbers against those calculated from the ideal gas law, however, showed that at these temperatures HG can be considered ideal; therefore, by adding the proper amount of HG to the system, contained in a fixed volume, we can achieve the desired number density required for HG.

General Information on Thallium Iodide

Thallium iodide is a diatomic molecule with a dissociation energy of 2.78 eV (Van Neen et al. 1980, p. 371). The melting point of TLI, 440°C (Table 4) is much higher than that of TL. Furthermore, the temperature for the proposed system will be slightly lower than this.

Table 3. Physical properties of mercury

Description of the constant	Value
Atomic number	80
Atomic weight	200.59 grams/mole
Melting point	-38.87°C
Boiling point	356.58°C
Van der Waal's a coefficient	2.318 $\frac{\text{liters}^2\text{-atom}}{\text{mole}^2}$
Van der Waal's b coefficient	0.03978 $\frac{\text{liters}}{\text{mole}}$
Ground state	6^1So
First metastable state	6^3Po
Second metastable state	6^3P1
Lifetime of 1st metastable state	≅ 125 nsecs
Lifetime of 2nd metastable state	--

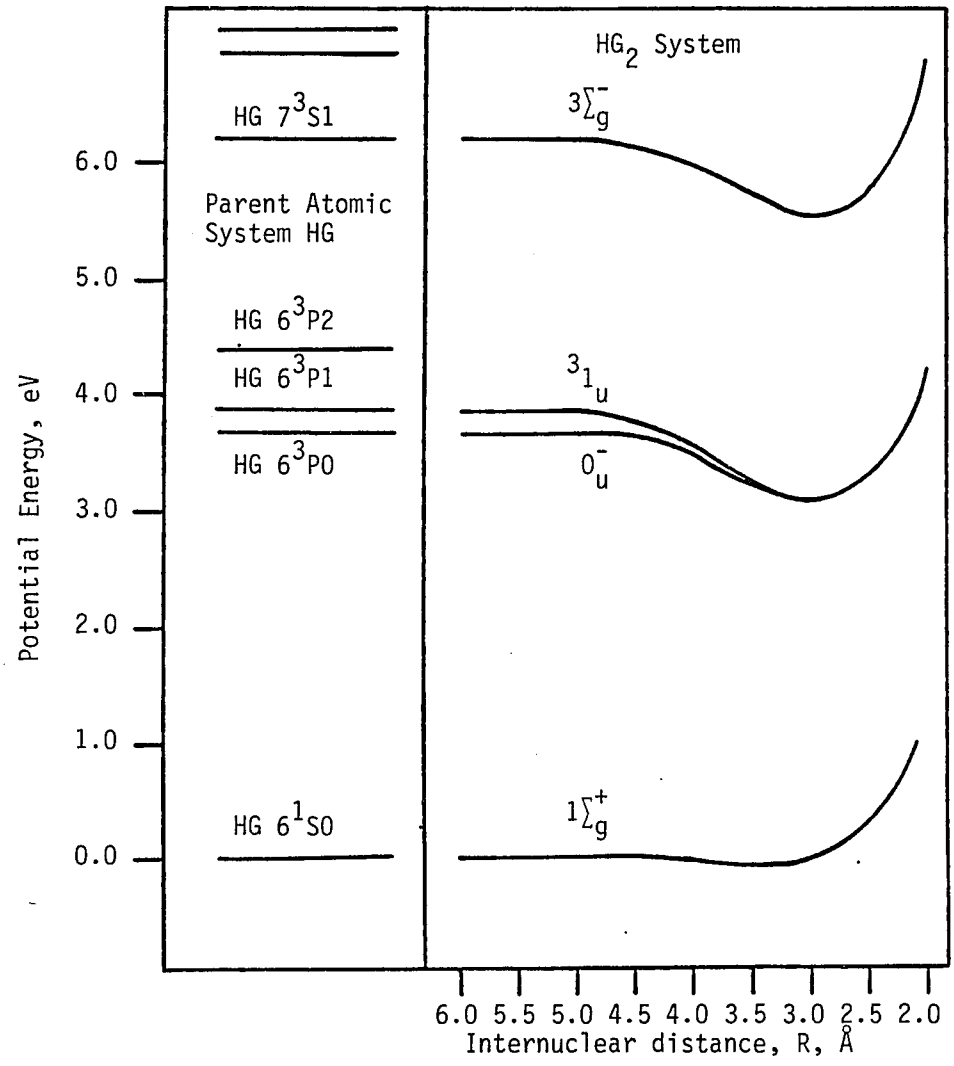

Figure 5. Energy level diagram for the HG_2 excimer system

Table 4. Physical properties of thallium iodide

Description of the constant	Value
Molecular weight	331.26 grams/mole
Melting point	440.0°C
Boiling point	824.0°C
Van der Waal's a coefficient	--
Van der Waal's b coefficient	--
Ground state	$^1\Sigma_0^+$
Dissociation energy (bond strength)	2.78 ± .02 eV
Re-attachment rate	1.8×10^{-10} cm^3/sec

Thus, the number density of TLI was calculated by the ideal gas law and the vapor pressure data of Rolsten (1961, pp. 267-268). Again, no information was available on Van der Waal's coefficients for TLI; however, the number densities calculated are in agreement with values used by others at approximately the same temperatures (Ludewigt et al. 1982, p. 143). Fluorescent data by Berkowitz and Chupka (1966, pp. 1287-93) suggest that the excited states of TLI are weakly bound or repulsive, with the exception of the state formed by TL^+ and I^- ions (see Figure 6). This is important, since metastable states would create possible quenching problems for our system. The reattachment rate for TLI being produced by TL and I ground state atoms is 1.8×10^{-10} cm^3/sec (Schlie et al. 1980, p. 4529). At this rate of formation, the generation of 10^{16} TLI molecules from TL and I would require several microseconds, which will limit the recycle time of the proposed system.

Photodissociation of Thallium Iodide into Excited Atomic Fragments

Photodissociation of thallium halides has been studied extensively by Van Neen (1980, pp. 371-84) and Maya (1979, pp. 579-93). The UV absorption cross section versus wavelength for TLI is shown in Figure 7 (Davidovits and Bellisio 1968, p. 3563). The region we will be dealing with for our model is the range between 1800 to 2100 Å. The other regions are discussed in detail by Davidovits and Bellisio, and will be examined later in Chapter 5. The apparent linear relationship between wavelength and the absorption cross section in the region below

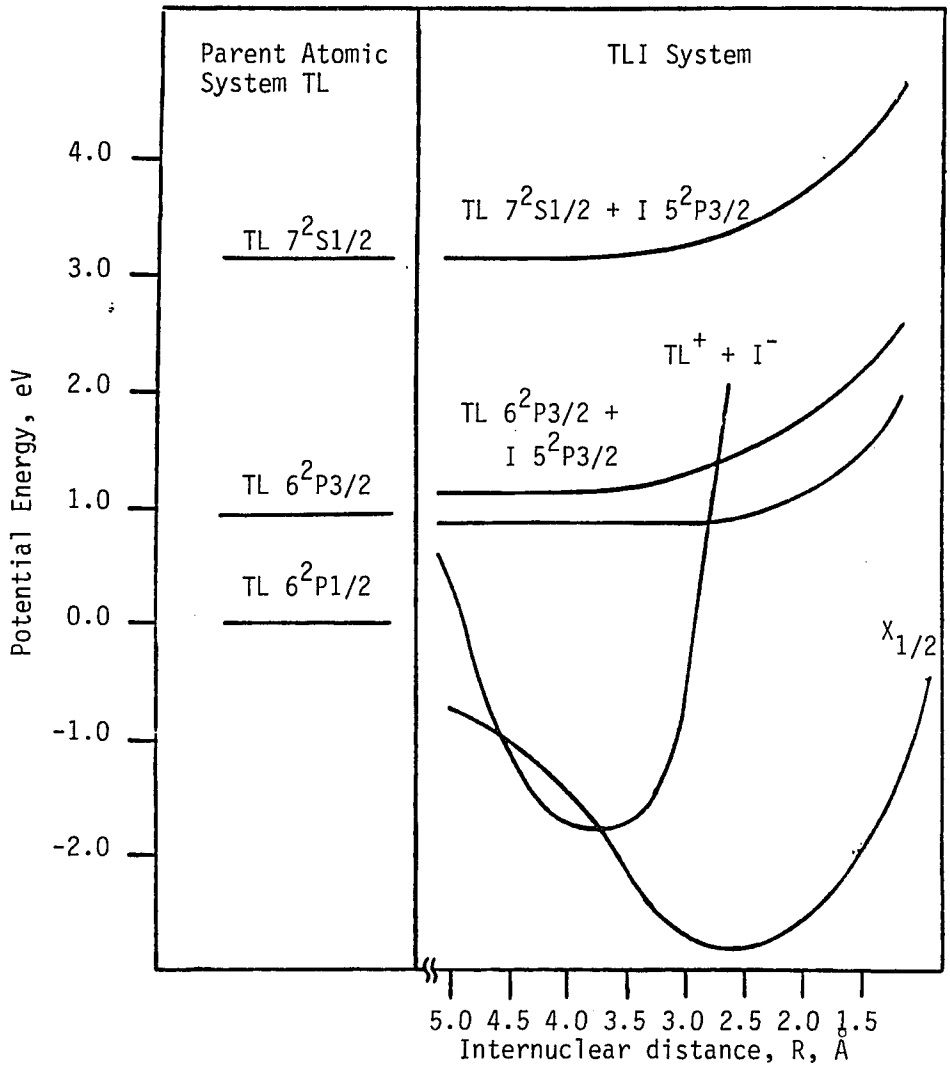

Figure 6. Energy level diagram for the TLI molecular system

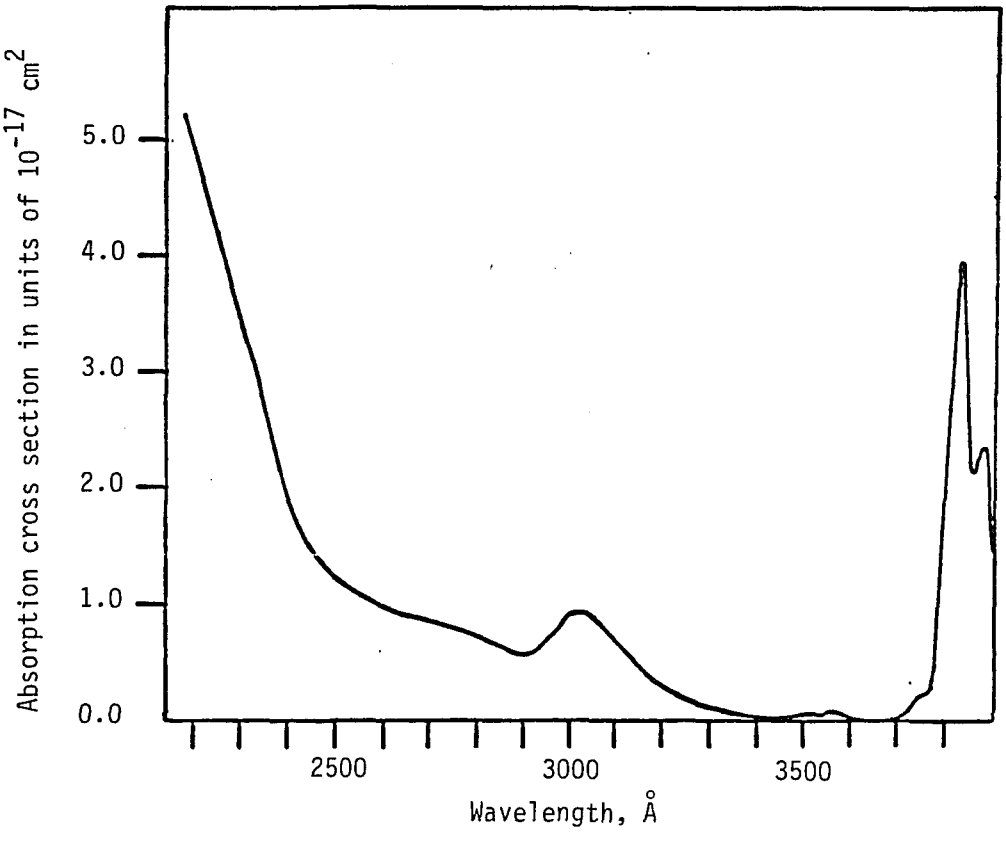

Figure 7. Absorption cross section for TLI

2100 Å was used to predict the absorption cross section at 1930 Å (the wavelength of our pump laser). This value, 7.4×10^{-17} cm^2, is in agreement with that calculated by Ehrlich et al. (1978, p. 931), who performed absorption experiments and used Beer's law, equation (3.3), to obtain the desired results:

$$I = I_0 e^{-\alpha z} \tag{3.3}$$

where I is the intensity (watts per area) of the incident beam traveling in direction z, with an absorption coefficient, α (per unit length). The wavelength of our pump laser (ARF excimer laser) is 193 nm. Several people have photodissociated TLI using photons at this wavelength to determine the efficiency of producing TL $7^2S1/2$ atoms per TLI molecule dissociated (Ehrlich et al. 1978, p. 931). The efficiency values obtained range from 35% to as high as 62%, with the hope of achieving 75% in the future. An additional support for these high efficiencies is the fact that ion formation as the result of photodissociation using 193 nm photons is minimal, as shown in Figure 8 (Berkowitz and Chupka 1966, p. 1289). The efficiency value used in the model was chosen to be 50%, which represents a compromise between the various quoted values.

Ehrlich et al. (1978, p. 932) investigated the speeds of the dissociated atoms after the dissociation using 193 nm photons. He found the speed of the TL $7^2S1/2$ atoms to be 2.5 times the Maxwell-Boltzmann speed for a TL atom in the ground state, having the system 's temperature, T. In Appendix A, I calculated a similar value for the

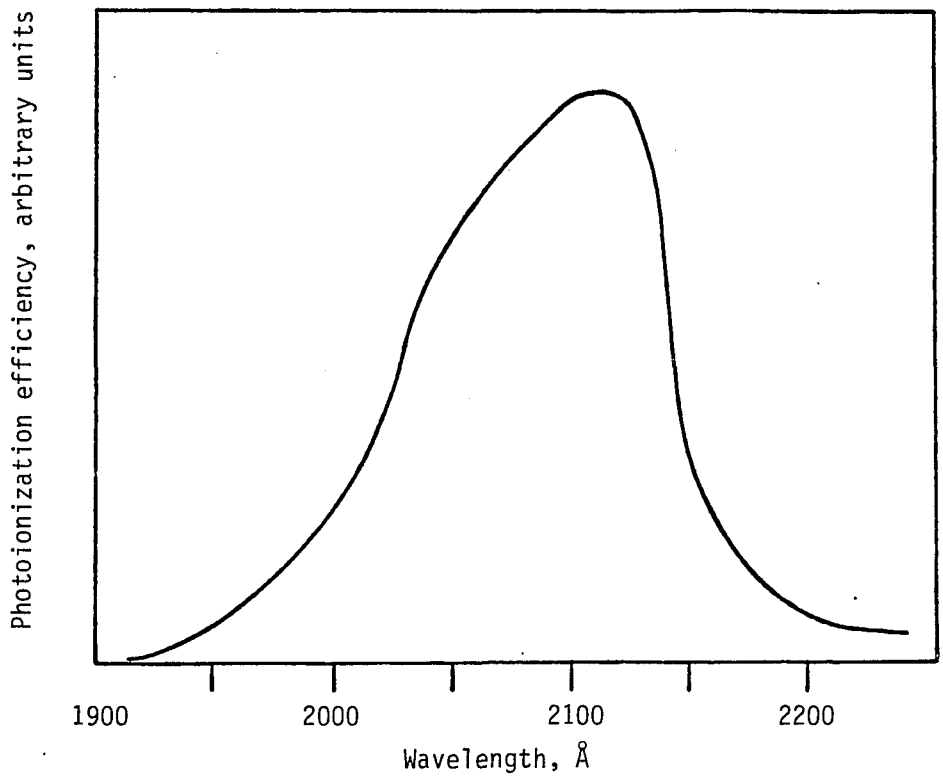

Figure 8. Photoionization efficiency curve of TLI for I^- formation

speed of the TL $7^2S1/2$ atom molecule, using classical mechanics. See Table 5 for the Maxwell-Boltzmann speeds of TL, TLI and HG, for the temperatures indicated. This excess kinetic energy poses the same problem as the high temperature requirements for TL did for the formation of $TLHG^*$; that is, the TL $7^2S1/2$ atoms must be "cooled" before they can combine with HG atoms to form $TLHG^*$. The addition of a buffer gas with a low index of refraction may be added to minimize this problem.

Conclusions

The advantages of using TLI instead of pure TL in the gas mixture are the following, in view of what has been discussed: The vapor pressure of TLI allows the temperature of the system to be lowered by 400°C. This eliminates many of the engineering problems caused by the high temperature requirement needed for TL vapor. In addition to this, the lower temperature improves the gain of the system and minimizes some losses due to the creation of "hot" atoms. The photodissociation method is also simple to employ, and the gas kinetics are far less complicated than those of discharge or e-beam systems. However, even though photodissociation produces excited TL atoms very efficiently, one pays a price for this. The loss of TL $7^2S1/2$ atoms due to stimulated emission may prevent a sufficient population inversion for the $TLHG^*$ system, and the resultant production of TL $6^2P3/2$ atoms from this, combined with the slow re-formation of TLI, forces us to accept a system which cannot give us a continuous output.

Table 5. Maxwell-Boltzmann mean velocities of thallium, thallium iodide and mercury

Temperature °C	Thallium #/cm^3	Thallium Iodide #/cm^3	Mercury #/cm^3
340.0	2.52×10^2	1.98×10^2	2.54×10^2
350.0	2.54×10^2	2.00×10^2	2.56×10^2
360.0	2.56×10^2	2.01×10^2	2.58×10^2
370.0	2.58×10^2	2.03×10^2	2.60×10^2
380.0	2.60×10^2	2.04×10^2	2.63×10^2
390.0	2.62×10^2	2.06×10^2	2.65×10^2
400.0	2.64×10^2	2.07×10^2	2.67×10^2
410.0	2.66×10^2	2.09×10^2	2.68×10^2
420.0	2.68×10^2	2.10×10^2	2.70×10^2
430.0	2.70×10^2	2.12×10^2	2.72×10^2
440.0	2.72×10^2	2.13×10^2	2.74×10^2

CHAPTER 4

THE GENERATION OF A POPULATION INVERSION FOR THALLIUM MERCURY

In the following sections, an examination of the various reactions which can occur between atomic and molecular species, in the thermal gas mixture, ensues. A set of equations is derived, which describe the system during photodissociation of TLI and production of $TLHG^*$, based upon the assumptions dealing with the time duration of the laser pump pulse and the kinetics of the gas mixture. Finally, an analysis of the pumping method is performed, using computer aided numerical analysis techniques for variations of several parameters.

The General Pumping Scheme

The thermal gas mixture, for reasons discussed in Chapter 3, is composed initially of TLI and HG. First, photodissociation of TLI molecules occurs by the absorption of photons (λ = 193 nm) from the pump laser (ARF excimer laser), causing excitation of TLI molecules into higher (repulsive) states. Within a vibrational lifetime, the unstable TLI molecules dissociate into excited TL and I fragments. A certain percentage of the TL atoms are in the $7^2S1/2$ state. These atoms may go through radiative transitions (spontaneous or stimulated) to lower TL states, which represent a loss to the formation of $TLHG^*$. Those TL $7^2S1/2$ atoms that survive combine with HG atoms (in their ground state) by three body collisions to form $TLHG^*$. These excimers

can dissociate via collisions or undergo spontaneous emission to a repulsive state. Our model describes the events up to this point and answers the following question: "How many TLHG* molecules will be available for stimulated emission, to eventually cause a lasing action?" When a radiative transition does occur, after sufficient vibrational relaxation of the excimer, by either spontaneous or stimulated emission, the TLHG molecule will eventually dissociate into TL and I atoms in either their ground states or their first excited states. Those TL and I atoms in their first excited states must be deexcited, primarily by collisional processes. Then, TLI can be formed by TL and I atoms in their ground state, and the process can be repeated.

Densities, Kinetics and Absorptive Properties of the Gas Mixture

In all laser systems a threshold population inversion must be generated and maintained to cause a lasing action in the system. This inversion (threshold number density) is determined by equating the total gain of the system to the total loss of the system:

$$G(\nu) = \alpha(\nu) + \frac{1}{2L} \ln\left(\frac{1}{R_1 R_2}\right) \tag{4.1}$$

where $G(\nu)$ is the gain coefficient for the lasing species, $\alpha(\nu)$ represents the losses caused by the medium (gas mixture), L is the length of the laser cavity, and R_1, R_2 are the reflectivities of the mirrors used in the system. The major concerns are $G(\nu)$ and $\alpha(\nu)$; they determine the length of the cavity and the mirrors used to satisfy the

requirements indicated by equation (4.1). However, if the losses are too high, the system may not lase even if it is has a large gain. Gain, $G(\nu)$, and losses $\alpha(\nu)$, are determined by the gas densities, kinetics and absorptive qualities of the system. Using equation (2.16), we can calculate the threshold number density of the lasing species if we are given the threshold gain for lasing at frequency ν.

Drummond and Schlie (1976, pp. 3454-63) used a modified version of equation (2.15) to calculate the gain of the TLHG excimer system for specific densities of TL $7^2S1/2$ and HG, as ascertained from fluorescent data (see Figure 9). Note, however, that the system did not lase! If, for the moment, we were to consider this to be the gain for the TLHG excimer system and use equation (2.15) to calcualte the inversion densities for the radiative transitions λ = 459 nm and λ = 656 nm, the inversion density required for either transition would be approximately 10^{14} TLHG excimers per cubic centimeter. This number density is predicted to be the approximate threshold inversion density for several proposed excimer systems (Shahdin et al. 1981 p. 1278). This may or may not be the case for TLHG, but it can be used to predict, with some confidence, the lower limit of TLI and HG number densities needed to produce 10^{14} $TLHG^*$ per cubic centimeter, which is known to be necessary to cause superfluorescent emission (Drummond and Schlie 1976, pp. 3454-63). For excimer densities lower than this no strong emission is seen, and the population inversion would be insufficient for TLHG to lase. Therefore, what we are really looking at is the lower limit of a range

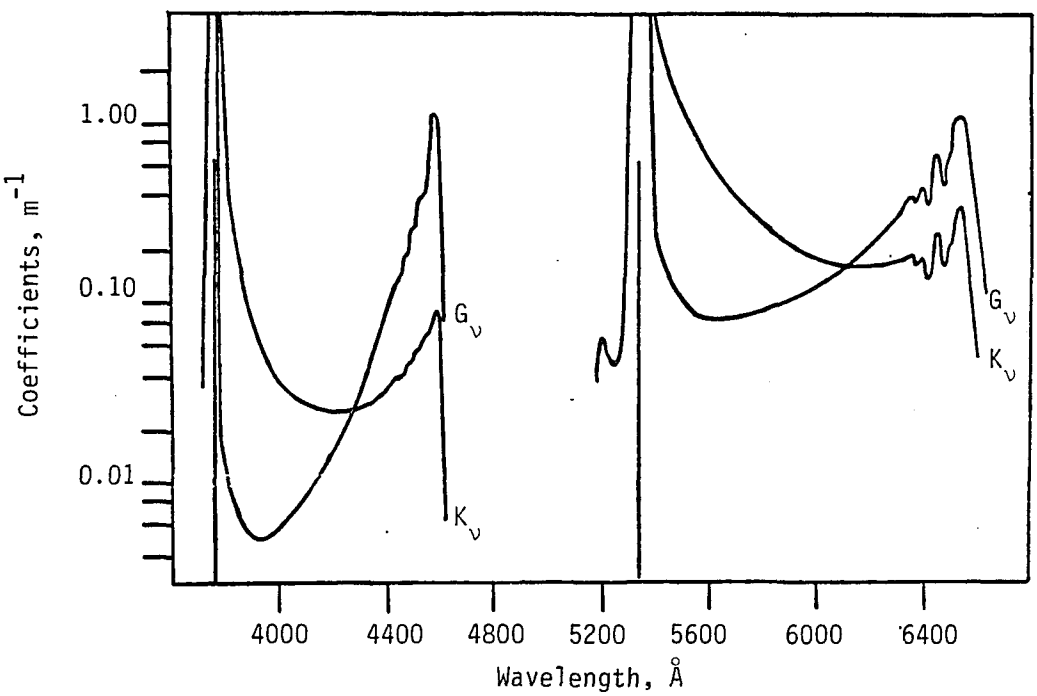

Figure 9. Absorption, K_ν, and stimulated emission, G_ν, coefficients for TLHG excimer bands.

of densities thought to be necessary for TLHG to lase, provided losses can be minimized and pumping mechanisms improved.

The upper limit for this range is determined by $\alpha(\nu)$. The TLHG excimer is formed by 3-body collisions using two HG atoms, but these atoms can also dissociate the excimer into TL and HG atoms. Because there are only so many TL $7^2S1/2$ atoms to combine with HG atoms (the formation rate depends on $[HG]^2$), an increase in [HG] above a certain range would only cause increases in collisional and absorptive losses for the system. The upper limit for the temperature determined TLI number density is also determined by $\alpha(\nu)$. Collisional processes involving TL and I atomic fragments and TLI molecules can de-excite TL $7^2S1/2$ atoms and TLHG excimers. In addition, the desired absorptive properties of the system may be degraded (Schlie et al. 1980, p. 4539). Thus, limiting the amount of TLI molecules present can minimize these quenching and absorption problems, hopefully without decreasing the gain for $TLHG^*$. See Table 6 for a listing of the various reactions which can occur in an optically excited TLI-HG gas thermal gas mixture. Note the many undesirable quenching processes (Schlie et al. 1980, p. 4540).

The suggested number density for TLI is $10^{16}/cm^3$ (Drummond and Schlie 1976, p. 3454; Ludewigt et al. 182, p. 143). This allows for the production of a sufficient number of TL $7^2S1/2$ atoms because of the large photon absorption cross section for TLI at λ = 193 nm (determined at the same TLI densities) and the available power per unit area in the short pulse typical of commercial excimer lasers operating at λ = 193

Table 6. Possible reactions in a thallium iodide-mercury gas mixture (TLI - thallium iodide, HG = mercury)

Reactants	Products
$TLI + h\nu$	$TL^+ + I^-$
$TL(6^2P3/2) + HG/HG_2$	$TL(6^2P1/2) + HG/HG_2$
$TL(6^2P3/2) + HG^*/HG_2^*$	$TL(7^2S1/2) + HG/HG_2$
$TLHG^* + HG$	$TL + HG_2^*$
$TLI + h\nu$	$TL(7^2S1/2) + I(5^2P1/2)$
$TLI + h\nu$	$TL(6^2D3/2,5/2) + I(5^2P1/2)$
$TL(6^2P3/2)$	$TL(6^2P1/2) + h\nu$ (λ = 1.28 μm)
$TL(7^2S1/2)$	$TL(6^2P3/2) + h\nu$ (λ = 535 nm)
$TL(7^2S1/2)$	$TL(6^2P1/2) + h\nu$ (λ = 377 nm)
$TL(6^2D3/2,5/2)$	$TL(6^2P3/2) + h\nu$ (λ = 351 nm)
$TL(6^2P3/2) + I(5^2P3/2)$	$TL(6^2P1/2) + I(5^2P1/2)$
$I(5^2P1/2)$	$I(5^2P3/2) + h\nu$ (λ = 1.315 μm)
$2I(5^2P3/2) + I_2$	$2I_2$
$TL(6^2P1/2) + I_2$	TLI + I
$TL(7^2S1/2) + TLI$	$TL(6^2P1/2) + TLI$
$TL(7^2S1/2) + I_2$	$TL(6^2P1/2) + I_2$
$TL(6^2P3/2) + TLI$	$TL(6^2P1/2) + TLI$
$TL(6^2P3/2) + I_2$	$TL(6^2P1/2) + I_2$
$TL(6^2P3/2) + TL(6^2P1/2)$	$2TL(6^2P1/2)$
$I(5^2P1/2) + I_2$	$I(5^2P3/2) + I_2$
$TLHG^* + HG$	$TL(7^2S1/2) + 2HG$

nm. The temperature required to produce this TLI number density is 430°C, which is below the melting point of TLI. Solid TLI is easier to work with, and the lower temperature improves the gain and kinetics of the system. Because we are considering short pulse (10 - 20 nsecs) excitation of the gas mixture, the TLI and photodissociated fragments will only collide with HG atoms (much higher density) during the pulse. This eliminates most of the quenching problems for TL $7^2S1/2$ atoms due to collisional processes.

The lower limit for [HG] is determined by the formation rate constant of $TLHG^*$, 3.0×10^{-31} cm^6/sec. For this value of K_F, the minimum density for HG is approximately $5.0 \times 10^{18}/cm^3$, for [TLI] = $1.0 \times 10^{16}/cm^3$. Experimental work indicates the that upper limit for [HG] is $5.0 \times 10^{19}/cm^3$, the value where the generation of $TLHG^*$ levels off due to the problems previously discussed (Drummond and Schlie 1976, pp. 3454-63). The optimum value for [HG] is somewhere in the indicated range.

The kinetics for the formation of $TLHG^*$ have already been discussed, but what happens to the system after $TLHG^*$ radiates and the process is repeated? The reformation of TLI occurs by three different means; binary long range harpooning reactions, wall stabilized binary reactions, and three body gas-phase reactions involving a buffer gas. The reformation of TLI from collisional processes involving TL $6^2P1/2$ and I_2 by harpooning reactions was examined in detail by Gedeon, Edelstein and Davidovits (1971, p. 5171). They determined the collisional cross section for the process to be 1.05×10^{-14} cm^2.

Reformation of TLI at the walls of the cavity was investigated by Burnham (1977, p. 132). The use of HG in three body gas-phase reactions involving TL and I atoms has not been investigated. The important point to note is that the production of TLI, after $TLHG^*$ radiates, prevents the formation of I_2 and TL_2, using the processes described and, furthermore, allows TLI to be recycled many times, which is important for a sealed metal vapor system.

The problem as mentioned before is the long metastable lifetime of TL $6^2P3/2$ atoms. We must first de-excite these atoms before we can form TLI. The use of TLI and I_2 to de-excite atoms has been investigated by Gedeon et al. (1971, p. 5171) and Bellisio and Davidovits (1976, p. 3474); large cross sections for these collisions indicate the process can occur rapidly. The final factor for the reformation of TLI is the diffusion of TL and I atoms to the vessel walls. This process is affected by the large HG density. Ehrlich et al. (1978, p. 932) investigated TLI reformation after photodissociation (HG not present) and estimated the TL photodissociation laser could operate with a pump rate in the kilohertz range. Similar rates would be expected for the TLHG excimer laser. Note, that for the proposed model, we are considering 10 - 20 nsec laser pump pulses; therefore these kinetic processes occur well after $TLHG^*$ radiates, primarily because of TLI's initial density and low temperature.

Using the initial conditions indicated and the established kinetics of the system, absorption losses at $\lambda = 193$ nm are minimal, because TLI is the only strong absorber present at this wavelength.

Thallium absorption of $TLHG^*$ emitted photons is minimal, but HG excimers can absorb these photons. Drummond and Schlie (1976, p. 3459) investigated this problem and showed these losses to be small.

The Model

In lieu of what has previously been discussed, and the use of short pulse excitation, several approximations can be made for which a simplified rate equation model may be derived for the time dependent densities. This set of rate equations can then be integrated over time to calculate values for the gas densities, which will enable us to determine the effectiveness of the pumping process in generating the necessary inversion for the excimer system.

Because of the large densities for HG (as compared to TLI), we can treat [HG] as a constant. This is further supported by the small absorption by HG at λ = 193 nm and the low temperature of the system. Recall D_0 for TLI is 2.78 eV, which implies that initially only TLI and HG will be present in the cell, because the temperature is low enough so that collisional processes could not dissociate TLI or excite HG. The pump pulse duration is 10 nsecs; therefore, because the densities of TLI and atomic fragments are below $10^{16}/cm^3$, we can neglect the quenching processes involving these particles during the pump pulse. Also, the production of TLI during the pump pulse can be neglected, because its reformation time is in microseconds. Finally, if we neglect stimulated emission and absorption for TL atoms during the pump pulse, the rate equation model becomes the following:

$$\frac{d[TLI]}{dt} = \frac{-\sigma I}{h\nu}[TLI] \qquad (4.2)$$

$$\frac{d[TL\ 7^2S1/2]}{dt} = \frac{\alpha\sigma I}{h\nu}[TLI] - \frac{[TL\ 7^2S1/2]}{\tau} - K_F[HG]^2[TL\ 7^2S1/2] \qquad (4.3)$$

$$\frac{d[TLHG^*]}{dt} = K_F[HG]^2[TL\ 7^2S1/2] - \frac{[TLHG^*]}{\tau^*} - K_D[HG][TLHG^*] \qquad (4.4)$$

Equation (4.2) represents the loss of TLI molecules due to photodissociation, where σ, 7.402×10^{-17} cm^2, is the absorption cross section for TLI at frequency $\lambda = 1.554 \times 10^6$ ghz. We assume that when TLI is excited to a repulsive state it quickly dissociates into atomic fragments. In equation (4.3), the first term on the right-hand side shows the production of TL $7^2S1/2$ atoms where α, 0.5, (as discussed in Chapter 3) represents that fraction of TLI which photodissociates into TL $7^2S1/2$ atoms. The second term deals with the losses due to spontaneous emission of TL $7^2S1/2$ atoms to lower electronic states. The lifetime of this state is 7.5 nsecs, as determined by Gallagher and Lurio (1964, pp. A87-103) using level crossing and double-optical resonance techniques. Both methods gave results which were in agreement. The last term describes the loss of TL $7^2S1/2$ atoms in forming TLHG excimers. As noted before, the formation of $TLHG^*$ depends on $[HG]^2$. The molecular formation rate, K_F, 3.0×10^{-31} cm^6/sec, was determined by Drummond and Schlie (1976, p. 3458) by examining fluorescent data for low HG densities in a TL-HG metal vapor mixture excited by an electrical discharge. Because of the low HG density, the molecular spectral distribution is a result of spontaneous emission by $TLHG^*$.

From this distribution an "effective" rate can be calculated. Values similar to this have been calculated for $TLXE^*$ (Schlie et al. 1980, p. 4540), and for HG_2^* (Komine and Byer 1977, p. 2507), which are comparable systems. The first term of equation (4.4) shows the production of $TLHG^*$ just discussed. The second term represents losses due to spontaneous emission. The value of τ^*, 12 nsecs (Drummond and Schlie 1976, p. 3462), is similar to that of TLXE, 11 nsecs (Schlie et al. 1980, p. 4540), and is reasonable when we consider the discussion of Chapter 2 relating parent atomic lifetimes to excimer lifetimes. The last term represents collisional losses for $TLHG^*$, primarily due to HG. No effective value for K_D has been determined; however, the value is expected to be in the 10^{-10} to 10^{-12} cm^3/sec range. The model will be investigated for this range of K_D for various densities of HG. See Table 7 for a summary of the coefficients used in the model.

Results of the Analysis

The rate equations can be readily solved analytically by integrating equation (4.2) and plugging its solution into equation (4.3), etc. See Appendix B for the major steps involved in solving the model analytically, where the intensity, I, of the pump laser is treated as a constant. The system can also be solved using computer aided numerical analysis techniques. The use of DARE P (Wait 1977), a computer program which solves (by numerical integration) a set of differential equations in state variable form, provided the necessary information (data file) with minimal changes to the program's text file (see Appendix C) for each simulation of the model for various values of K_D and [HG]. Using

Table 7. Definitions and values of constants used in the model

Description of the constant	Value
σ) UV absorption cross section of TLI	7.4×10^{-17} cm^2 (λ = 193 nm)
I) Intensity of the laser pump	5.0×10^{7} $\frac{watts}{cm^2}$
τ) Lifetime of TL $7^2S1/2$ state	7.5 nsecs
K_F) 3 body formation rate constant for $TLHG^*$	3.0×10^{-31} $\frac{cm^6}{sec}$
α) % fraction of TLI which produces TL $7^2S1/2$	0.5
ν) Frequency of laser pump	1.554×10^{15} Hz
K_D) Dissociation rate constant for $TLHG^*$	1.0×10^{-9} - 1.0×10^{-12} $\frac{cm^3}{sec}$
τ^*) Lifetime of $TLHG^*$	12.0 nsecs
h) Planck's constant	6.6261×10^{-34} joule-sec

the CALCOMP plotter program package with 100 data points (1 point per 0.1 nsec division) for each time dependent number density, the graphs of Figures 10, 11, and 12 were created. See Tables 8, 9, 10 and 11 for the results of the simulations. The intensity of the laser pump for the simulation was treated as a constant because we are only considering physical effects during the 10 nsec pump pulse.

The maximum $TLHG^*$ densities achieved for a given value of K_D and [HG] where [TLI] = $10^{16}/cm^3$, are listed in Table 11. Because the model does not take into account losses due to TL $7^2S1/2$ stimulated emission, it is evident that for HG densities below 1 x $10^{19}/cm^3$, where the maximum $TLHG^*$ is 2.29 x $10^{14}/cm^3$, an insufficient population inversion is generated. This is further supported by the fact that both $TLHG^*$ radiative transitions require at least an inversion of $10^{14}/cm^3$ in order for net stimulated emission to occur. For [HG] = 2.5 x $10^{19}/cm^3$, large inversion densities are achieved for values of K_D less than or equal to 5.0 x 10^{-11} cm^3/sec. Figures 10, 11 and 12 show the densities versus time for values of K_D in this range, where the [HG] = 2.5 x $10^{19}/cm^3$. The values of K_D for similar excimer systems are in this 5.0 x 10^{-11} cm^3/sec to 5.0 x 10^{-12} cm^3/sec range (Shahdin et al. 1981, p. 1280; Rhodes 1984, pp. 196-197).

For larger values of K_D, the time it takes for $[TLHG^*]$ to reach a maximum is shorter, but this provides no real benefit to the system, as indicated by a comparison of the graphs. However, the earlier $[TLHG^*]$ reaches its maximum value the better, because it prevents losses from TL $7^2S1/2$ stimulated emission. As indicated, the time

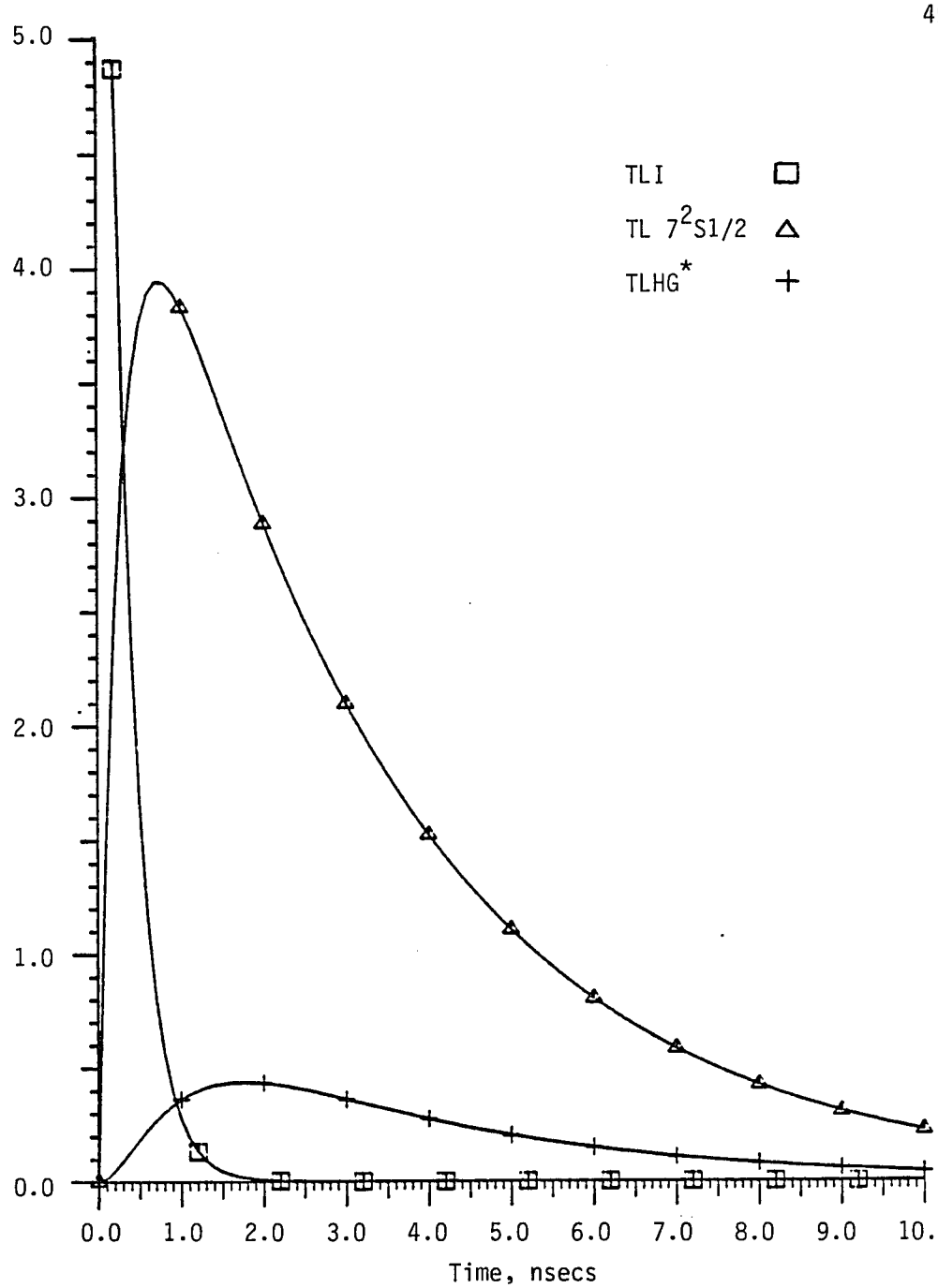

Figure 10. Graph of TLI, TL $7^2S1/2$, $TLHG^*$ number densities versus time for $K_D = 5.0 \times 10^{-11}$ cm^3/sec and [HG] = 2.5×10^{19}/cm^3

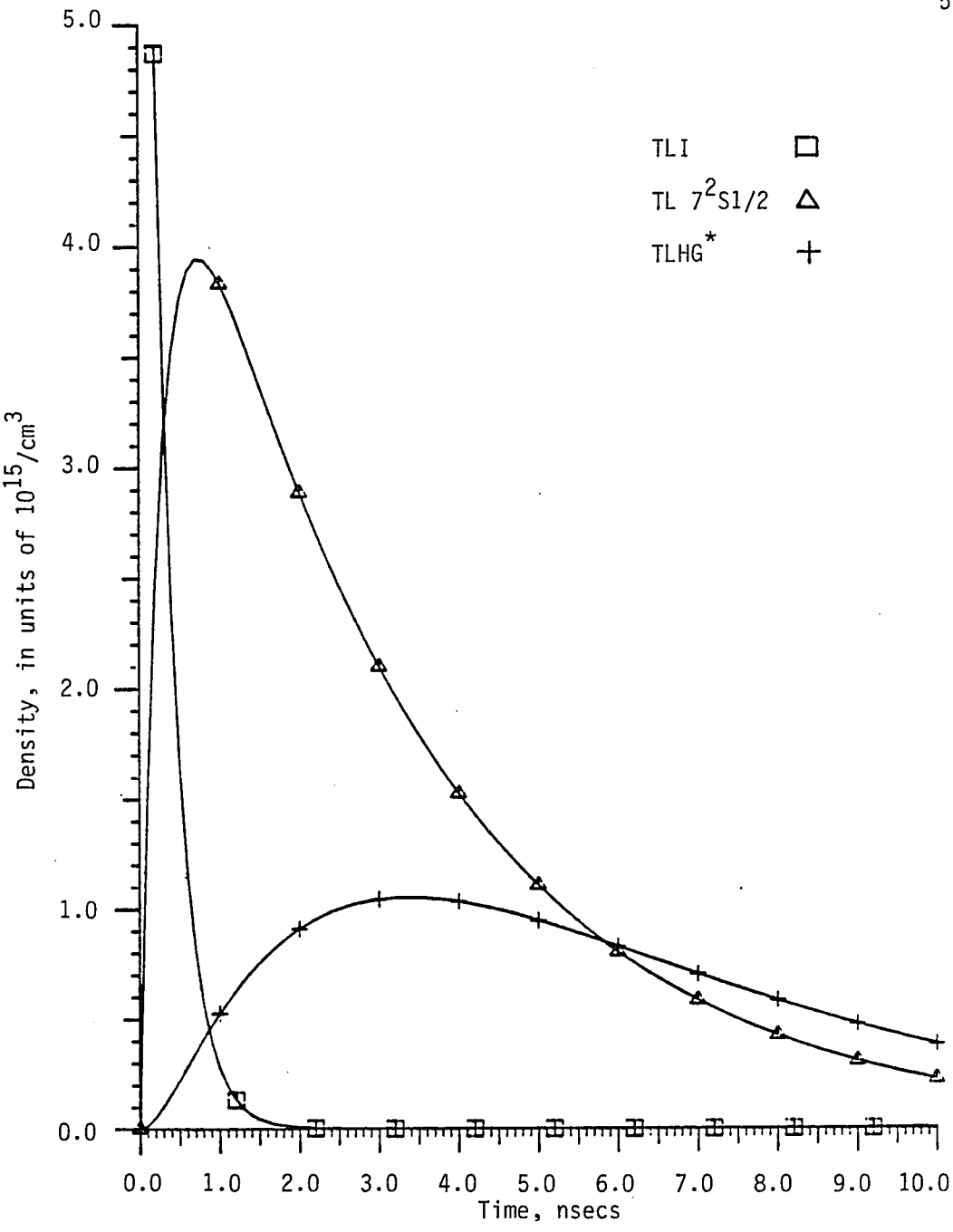

Figure 11. Graph of TLI, TL $7^2S1/2$, TLHG* number densities versus time for $K_D = 1.0 \times 10^{-11}$ cm^3/sec and $[HG] = 2.5 \times 10^{19}/cm^3$

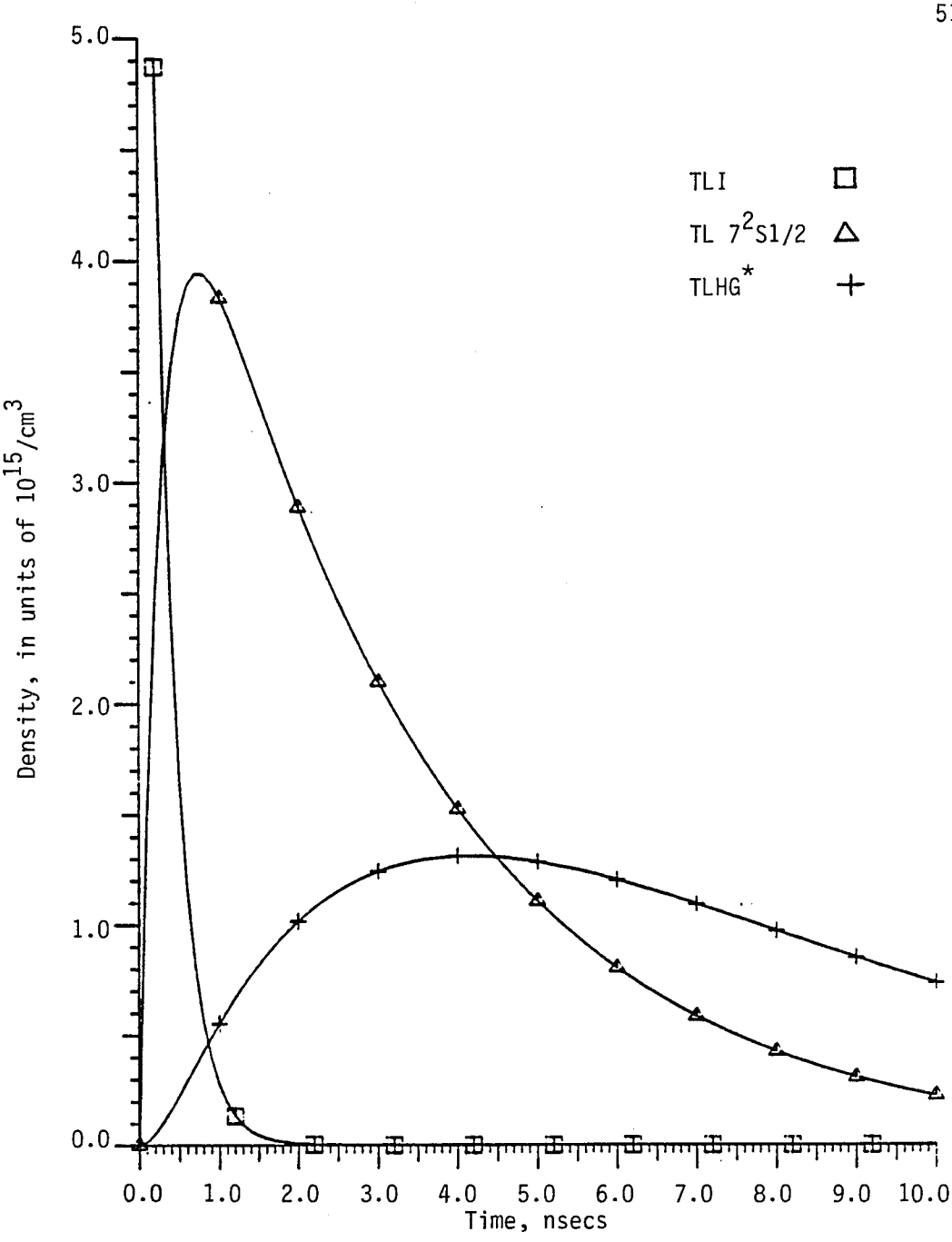

Figure 12. Graph of TLI, TL $7^2S1/2$, TLHG* number densities versus time for $K_D = 5.0 \times 10^{-12}$ cm^3/sec and $[HG] = 2.5 \times 10^{19}/cm^3$

Table 8. Time dependent number densities predicted by the model for $K_D = 5.0 \times 10^{-11}$ cm^3/sec and $[HG] = 2.5 \times 10^{19}/cm^3$

Time nsecs	TLI #/cm^3	TL $7^2S1/2$ #/cm^3	TLHG* #/cm^3
0.0	1.00×10^{16}	0.0	0.0
1.0	2.74×10^{14}	3.83×10^{15}	3.62×10^{14}
2.0	7.53×10^{12}	2.89×10^{15}	4.33×10^{14}
3.0	2.07×10^{11}	2.10×10^{15}	3.70×10^{14}
4.0	5.67×10^{9}	1.52×10^{15}	2.75×10^{14}
5.0	1.56×10^{8}	1.10×10^{15}	2.03×10^{14}
6.0	4.27×10^{6}	8.01×10^{14}	1.48×10^{14}
7.0	1.17×10^{5}	5.81×10^{14}	1.07×10^{14}
8.0	3.22×10^{3}	4.22×10^{14}	7.80×10^{13}
9.0	8.83×10^{1}	3.06×10^{14}	5.66×10^{13}
10.0	2.42×10^{0}	2.22×10^{14}	4.11×10^{13}

Table 9. Time dependent number densities predicted by the model for $K_D = 1.0 \times 10^{-11}$ cm^3/sec and [HG] = 2.5×10^{19}/cm^3

Time nsecs	TLI #/cm^3	TL $7^2S1/2$ #/cm^3	TLHG* #/cm^3
0.0	1.0×10^{16}	0.0	0.0
1.0	2.74×10^{14}	3.83×10^{15}	5.25×10^{14}
2.0	7.53×10^{12}	2.89×10^{15}	9.08×10^{14}
3.0	2.07×10^{11}	2.10×10^{15}	1.04×10^{15}
4.0	5.67×10^{9}	1.52×10^{15}	1.03×10^{15}
5.0	1.56×10^{8}	1.10×10^{15}	9.44×10^{14}
6.0	4.27×10^{6}	8.01×10^{14}	8.25×10^{14}
7.0	1.17×10^{5}	5.81×10^{14}	7.00×10^{14}
8.0	3.22×10^{3}	4.22×10^{14}	5.80×10^{14}
9.0	8.83×10^{1}	3.06×10^{14}	4.72×10^{14}
10.0	2.42×10^{0}	2.22×10^{14}	3.80×10^{14}

Table 10. Time dependent number densities predicted by the model for $K_D = 5.0 \times 10^{-12}$ cm^3/sec and [HG] = 2.5×10^{19}/cm^3

Time nsecs	TLI_3 #/cm^3	TL $7^2S_{1/2}$ #/cm^3	$TLHG_3^*$ #/cm^3
0.0	1.0×10^{16}	0.0	0.0
1.0	2.74×10^{14}	3.83×10^{15}	5.52×10^{14}
2.0	7.53×10^{12}	2.89×10^{15}	1.02×10^{15}
3.0	2.07×10^{11}	2.10×10^{15}	1.24×10^{15}
4.0	5.67×10^{9}	1.52×10^{15}	1.31×10^{15}
5.0	1.56×10^{8}	1.10×10^{15}	1.28×10^{15}
6.0	4.27×10^{6}	8.01×10^{15}	1.20×10^{15}
7.0	1.17×10^{5}	5.81×10^{15}	1.09×10^{15}
8.0	3.22×10^{3}	4.22×10^{14}	9.68×10^{14}
9.0	8.83×10^{1}	3.06×10^{14}	8.47×10^{14}
10.0	2.42×10^{0}	2.22×10^{14}	7.32×10^{14}

Table 11. Maximum [TLHG*] number densities achieved for various values of K_D and [HG]

Time to reach max TLHG* densities nsecs	K_D cm^3/sec	[HG] $\#/cm^3$	[TLHG*] $\#/cm^3$
1.6	$5. \times 10^{-10}$	5.0×10^{18}	1.20×10^{13}
3.5	$1. \times 10^{-10}$	5.0×10^{18}	4.07×10^{13}
4.8	$5. \times 10^{-11}$	5.0×10^{18}	5.98×10^{13}
7.6	$1. \times 10^{-11}$	5.0×10^{18}	1.01×10^{14}
8.4	$5. \times 10^{-12}$	5.0×10^{18}	1.11×10^{14}
1.3	$5. \times 10^{-10}$	7.5×10^{18}	1.86×10^{13}
2.8	$1. \times 10^{-10}$	7.5×10^{18}	6.90×10^{13}
3.9	$5. \times 10^{-11}$	7.5×10^{18}	1.07×10^{14}
6.8	$1. \times 10^{-11}$	7.5×10^{18}	2.01×10^{14}
7.7	$5. \times 10^{-12}$	7.5×10^{18}	2.29×10^{14}
1.2	$5. \times 10^{-10}$	1.0×10^{19}	2.50×10^{13}
2.4	$1. \times 10^{-10}$	1.0×10^{19}	9.81×10^{13}
3.3	$5. \times 10^{-11}$	1.0×10^{19}	1.56×10^{14}
6.1	$1. \times 10^{-11}$	1.0×10^{19}	3.18×10^{14}
7.1	$5. \times 10^{-12}$	1.0×10^{19}	3.72×10^{13}
0.8	$5. \times 10^{-10}$	2.5×10^{19}	5.85×10^{13}
1.3	$1. \times 10^{-10}$	2.5×10^{19}	2.58×10^{14}
1.8	$5. \times 10^{-11}$	2.5×10^{19}	4.38×10^{14}
3.4	$1. \times 10^{-11}$	2.5×10^{19}	1.05×10^{15}
4.1	$5. \times 10^{-12}$	2.5×10^{19}	1.31×10^{15}

required for the maximum [TLHG*] is 4.1 nsecs, which is well within the lifetime of the TL $7^2S1/2$ state, therefore spontaneous emission losses are minimal.

For larger values of [HG] the model is inadequate, as indicated earlier by the work done by Drummond and Schlie (1976, p. 3454), but the simulations confirm the initial metal vapor densities suggested by them for the proposed system.

CHAPTER 5

CONCLUSIONS

Experimental work has been done using the proposed pumping scheme. The resultant data is compared to that of this work, and conclusions are drawn. Improvements for this system are discussed, including suggestions for future experimental work. Photodissociation using other pump wavelengths is briefly examined, and, finally the paper concludes with a few words on the pumping schemes proposed.

Suggestions to Improve the Method Employed

It is evident from the data that we would, if the system were built, expect to see superfluorescent emission from $TLHG^*$, provided K_D is small enough. However, this is not the case. Ludewidgt et al. (1982 pp. 143-47) did the experiment using the proposed system, and only weak $TLHG^*$ emission was observed for optical excitation at λ = 193 nm. Either K_D or stimulated emission losses from TL (not included in the model) prevented the generation of a large inversion for $TLHG^*$. Because superfluorescent emission was observed using different pump wavelengths, we conclude that stimulated emission by TL is the major loss mechanism. One suggestion by Drummond and Schlie (1976, p. 3463), is the addition of a low index of refraction buffer gas. This will improve the thermalization of "hot" TL $7^2S1/2$ atoms by removing their excess kinetic energy. It will also increase the formation rate of

$TLHG^*$ by collisional vibrational relaxation of the excimer during formation. The experiment discussed did not use a buffer gas in the system. The gas mixture should be examined at several temperatures and densities for the buffer gas to maximize this effect.

Alternative Methods Using Photodissociation

Another way to minimize TL stimulated emission losses is that of simultaneous production of excited and ground state TL atoms. This will reduce the TL inversion (shown in the data) and thus inhibit stimulated emission. Ludewidgt et al. (1982, pp. 143-47) did just that by using pump wavelengths, λ = 351 nm and λ = 249 nm. It was first thought that a two photon process produced TL $6^2P3/2,1/2$ states by photodissociation of TLI and subsequent absorption of another photon by these states produced, in turn, TL $7^2S1/2$ states, as is the case for INBR and INCL (Cool and Koffend 1980, pp. 2287-91). However, though this may occcur, the process actually involved the excitation (by pump photons) of HG to form HG_2^* and HG^*, which caused strong emission by both TL^* and $TLHG^*$. The excited HG atoms and molecules collided with the TL $6^2P3/2$ atoms to produce TL $7^2S1/2$ atoms in sufficient quantity to generate a large inversion for $TLHG^*$, while minimizing the emission losses by TL^*. It has been shown that the cross section for this reaction is on the order of 10^{-14} cm^2, while the reverse reaction involving $TLHG^*$ and HG has a cross section of 10^{16} cm^2 (Hamil et al. 1979, p. 639). Future work on these formation rates for various pump times and system temperatures, with the addition of a buffer gas, need

to be done for one to optimize the set of parameters necessary for the best possible output.

Future Outlook

Using a gas mixture suggested by the model proposed in this thesis, we have the conditions necessary to implement the TL photodissociation laser (Ehrlich et al. 1978, p. 931). By improving the kinetics of the system and using the excitation of HG atoms, a lasing action for the $TLHG^*$ system seems feasible using the technically clean photodissociative method. The possible use of excimer flashlamps to pump the system has yet to be investigated, but future work in this area may lead to a compact efficient $TLHG^*$ laser.

APPENDIX A

CALCULATION OF THE SPEED OF A TL $7^2S1/2$ ATOM RESULTING FROM PHOTODISSOCIATION OF A TLI MOLECULE IN THE GROUND STATE

The question I wish to answer is "What is the speed of a TL $7^2S1/2$ atom as a result of a photon of frequency λ colliding with a TLI molecule, causing a dissociation of the molecule into specific atomic fragments?" To answer this question I will consider (classically) a stationary TLI molecule (center of momentum frame for TLI) at temperature, T, with a total mass, M_{TLI}. The alignment of the molecule is such that the internuclear axis connecting the TL and I atoms is parallel to the x axis. The colliding photon has a momentum, $\hbar k$, in the positive x direction. The collision is considered to be instantaneous and inelastic.

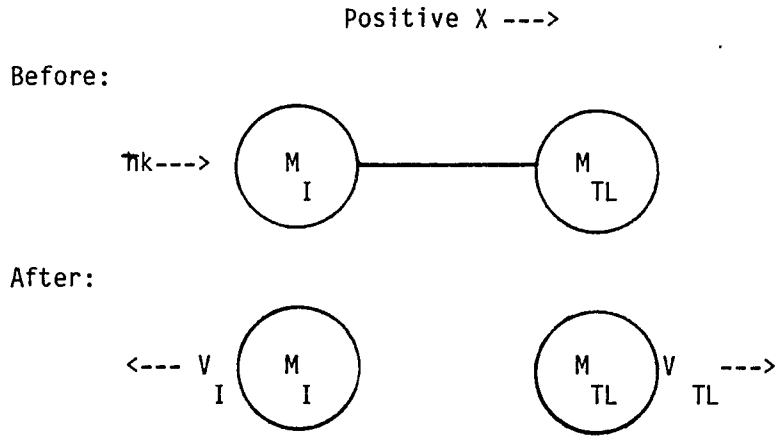

All the photon's energy is absorbed by the molecule. This situation leads to the following set of equations for conservation of energy and momentum:

$$\hbar\omega + E_{INT}[TLI] = E_T[TL] + E_T[I] + E_{INT}[TL] + E_{INT}[I] + D_o \quad (A.1)$$

$$\hbar k = M_{TL}V_{TL} + M_I V_I \quad (A.2)$$

where $E_{INT}[TLI]$ is the internal energy of the TLI molecule before the collision and E_T is the kinetic energy of the TL atom after the collision, etc. D_o is the dissociation energy (bond strength) of the TLI molecule. Since hk is insignificant compared to the momentum of either atom, equation 2 becomes:

$$M_{TL}V_{TL} = -M_I V_I \quad (A.3)$$

The equipartition theory states the average internal energy of a diatomic molecule at a given temperature is 2kT, one kT for its vibrational energy and one kT for its rotational energy. Because we are considering the production of TL $7^2S1/2$ atoms, by energy conservation, the I atom must be in its ground state, with zero internal energy; hence, $E_{INT}[TL] = E_{INT}[TL\ 7^2S1/2]$, and $E_{INT}[I] = 0$. Substituting the above values into equation 1 and combining with equation 3 yields the following equation for V_{TL}^2, where D_o for TLI is 2.78 eV:

$$V_{TL}^2 = \frac{2[h\omega + 2kT - E_{INT}[TL\ 7^2S1/2] - D_o]}{M_{TL} + M_{TL}^2/M_I^2} \quad (A.4)$$

This equation (taking the square root) yields the speed for the TL $7^2S1/2$ atom.

The result of this derivation gives us the average speed of TL $7^2S1/2$ atoms (in the center of momentum frame for TLI) in a thermal gas mixture which is isotropic (TLI molecules have no preferred orientation before dissociation, and the photon's momentum is negligble); in this case a macroscopic statistical treatment is valid. Converting this center of momentum speed to the lab frame is done by adding this speed to the Maxwell-Boltzmann average speed of the TLI molecule at a given temperature. The sum is the statistical average speed of the TL $7^2S1/2$ atoms resulting from the photodissociation of the TLI molecules. This yields a speed which is roughly 2.5 times the Maxwell-Boltzmann average speed of a TL atom in the ground state at the same temperature (see Table 5). Note the speed of the TL $7^2S1/2$ atoms resulting from photodissociation of TLI can also be determined by examining the doppler broadened profiles for electronic radiative transitions emanating from the TL $7^2S1/2$ state (Ehrlich et al. 1978, p. 932). This value then can be used in the previously discussed equations to determine D_0 for TLI (Kawasaki, Litvak and Bershon 1976, pp. 1434-37).

APPENDIX B

ANALYTICAL SOLUTION TO THE MODEL EQUATIONS

Because of the approximations made, as discussed in Chapter 4, the model that describes the production of $TLHG^*$ molecules by the photodissociation of TLI molecules reduces to a set of three first order differential equations. A brief description of the constants used in the model including their numerical values is given in Table 7. For a more detailed discussion about each constant with references please refer back to Chapter 4. Keeping in mind that the densities of TLI, TL $7^2S1/2$ and $TLHG^*$ are the only time dependent quantities in the model, with the possible exception of I, the intensity of the laser pump, the model equations are as follows:

$$\frac{d[TLI]}{dt} = \frac{\sigma I[TLI]}{h\nu} \tag{B.1}$$

$$\frac{d[TL\ 7^2S1/2]}{dt} = \frac{\alpha\sigma I[TLI]}{h\nu} - \frac{[TL\ 7^2S1/2]}{\tau} - K_F[TL\ 7^2S1/2][HG]^2 \tag{B.2}$$

$$\frac{d[TLHG^*]}{dt} = K_F[TL\ 7^2S1/2][HG]^2 - \frac{[TLHG^*]}{\tau^*} - K_D[TLHG^*][HG] \tag{B.3}$$

Because we are only considering time events during the laser pump pulse, we can treat the intensity, I, of the laser pump as a constant. This is a valid assumption in practice, but one has to consider the

rise time for the pump pulse. The current advances in laser technology indicate that rise time is not a problem, nor is stability of the laser pump. This assumption allows us to solve equation (B.1) and use its solution to solve equation (B.2). The solution to equation (B.2) can then be used to solve equation (B.3). Solving equation (B.1) yields an exponential time dependence for [TLI].

$$[TLI] = [TLI]_0 \exp[-I\sigma t/h\nu] \tag{B.4}$$

Plugging equation (B.4) into equation (B.2) and using Laplace transform techniques produces a solution for [TL $7^2S1/2$], which, as we should expect, is a combination of time dependent exponentials.

$$[TL\ 7^2S1/2] = \frac{\alpha\sigma I[TLI]_0}{h\nu} \cdot \left[\frac{\exp(-I\sigma t/h\nu) - \exp(-[1/\tau + K_F[HG]^2]t)}{1/\tau + K_F[HG]^2 - \sigma I/h\nu} \right] \tag{B.5}$$

Finally, substituting equation (B.5) into equation (B.3) and using similar techniques in solving equation (B.2), we find the analytical solution for [$TLHG^*$] to be:

$$[TLHG^*] = \frac{\alpha\sigma I[TLI]_0 K_F[HG]^2}{h\nu} \cdot \left[\frac{\exp(-At)}{(B-A)(C-A)} + \frac{\exp(-Bt)}{(A-B)(C-B)} + \frac{\exp(-Ct)}{(A-C)(B-C)} \right] \tag{B.6}$$

where $A = K_D[HG] + 1/\tau^*$

$B = I\sigma/h\nu$

$C = 1/\tau + K_F[HG]^2$

Remember these solutions are only valid for the various densities during the pump pulse. We could treat the intensity as a pulse to examine times after the pulse, but the model is not adequate to describe the physical processes for those times.

APPENDIX C

DARE P TEXT FILE

```
*THIS IS A SET OF THREE PARTIALLY COUPLED FIRST ORDER DIFFERENTIAL
*EQUATIONS.  THE SOLUTION TO THESE EQUATIONS PROVIDES QUANTITATIVE
*INFORMATION CONCERNING THE GENERATION OF A POPULATION INVERSION FOR
*THE TLHG EXCIMER SYSTEM USING UV  PHOTODISSOCIATION OF TLI IN THE
*PRESENCE OF HG IN A THERMAL GAS MIXTURE.  TO PERFORM THE NUMERICAL
*COMPUTATION OF THE SOLUTION REQUIRES A DAREP FILE SIMILAR TO THIS
*ONE.  THE OUTPUT IS A DATA FILE WHICH CONTAINS REQUESTED INFORMA-
*ABOUT THE SOLVED EQUATIONS.
*
*
*DEFINITIONS
*
*
*  V  IS THE POPULATION DENSITY OF THE TLI GROUND STATE.
*  W  IS THE POPULATION DENSITY OF THE TL 7S1/2 STATE,(TL*).
*  Y  IS THE POPULATION DENSITY OF THE TLHG EXCIMER, (TLHG*).
*
*  A1 IS THE UV ABSORPTION CROSS SECTION OF TLI AT LAMDA=193NM
*     DIMENSIONS=CM**2
*  A2 IS THE INTENSITY OF THE LASER PUMP
*     DIMENSIONS=WATTS/CM**2
*  A3 IS THE SPONTANEOUS EMISSION LIFETIME OF THE TL 7S1/2 STATE
*     DIMENSIONS=SECS
*  A4 IS THE 3 BODY FORMATION RATE FOR TL*+2HG TO TLHG*+HG
*     DIMENSIONS=CM**6/SEC
*  A5 IS THE HG POPULATION DENSITY
*     DIMENSIONS=CM**-3
*  A6 IS THE FRACTION OF DISSOCIATED TLI WHICH PRODUCES TL 7S1/2
*     DIMENSIONS=NONE
*  A7 IS THE FREQUENCY OF THE LASER PUMP
*     DIMENSIONS=HERTZ
*  A8 IS THE DISSOCIATION RATE CONSTANT FOR TLHG*+HG TO TL 7S1/2+2HG
*     DIMENSIONS=CM**3/SEC
*  A9 IS THE SPONTANEOUS EMISSION LIFETIME OF THE TLHG EXCIMER
*     DIMENSIONS=SECS
*  B1 IS PLANCK'S CONSTANT
*     DIMENSIONS=JOULES-SEC
*
*
*USING DAREP REQUIRES THE EQUATIONS TO BE IN STATE VARIABLE FORM.
*THE FIRST DERIVATIVE WITH RESPECT TO TIME OF OUR THREE DEPENDENT
*VARIABLES IS DENOTED BY V.,W.,AND Y.,RESPECTIVELY.  THEREFORE
*OUR MODEL FOR THE POPULATION INVERSION IN DAREP FORM IS AS FOLLOWS:
*
*
 $D1
      V.=-((A1*A2)/(B1*A7))*V
      W.=((A6*A1*A2)/(B1*A7))*V-(W/A3)-(A4*A5*A5*W)
      Y.=(A4*A5*A5*W)-(Y/A9)-(A8*A5*Y)
END
*
```

```
*
*INITIAL CONDITIONS AND VALUES OF CONSTANTS
*
*
*MAXIMUM TIME OF LASER PUMP PULSE
*
      TMAX=10.E-9
*
*INTIAL DENSITY OF THE TLI VAPOR
*
       V=1.E16
*
*INITIAL DENSITY OF THE TL 7S1/2 STATE


*
       W=0.0
*
*INITIAL DENSITY OF THE TLHG EXCIMER
*
       Y=0.0
*
*VALUES OF THE PREVIOUSLY MENTIONED CONSTANTS USED IN THE MODEL
*
      A1=7.405E-17
      A2=5.E7
      A3=7.5E-9
      A4=3.E-31
      A5=5.E19
      A6=0.5
      A7=1.554E15
      A8=1.E-12
      A9=12.E-9
      B1=6.626176E-34
END
*
*
*OUTPUT OF VARIABLES IN TABLE AND GRAPH FORM VERSUS TIME IN
*INCREMENTS OF 0.1 NANOSECOND TIME PERIODS
*
*OUTPUT OF ALL THREE DEPENDENT VARIABLES VERSUS TIME IN TABLE FORM
*
LIST V,W,Y
*
*OUTPUT OF ALL THREE DEPENDENT VARIABLES VERSUS TIME IN GRAPH FORM
*WITH ALL THREE PLOTTED ON THE SAME GRAPH
*
PLOT V,W,Y
END
```

LIST OF REFERENCES

Berkowitz, J. and Chupka, W. A., "Photoionization of High-Temperature Vapors. I. The Iodides of Sodium, Magnesium and Thallium," J. Chem. Phys., 45 (1966), 1289.

Carbone, R. J. and Litvak, M. M., "Intense Mercury-Vapor Green Band Emission," J. Appl. Phys., 39 (1968), 2413-15.

Chemical Rubber Company, Handbook of Chemistry and Physics, 56th ed. (1975-76), D-176.

Cool, Torrill A. and Koffend, John B., "Two Photon Excitation of Indium Atoms by Photodissociation of InCl and InBr," J. Chem. Phys., 74 (1981), 2287-91.

Davidovits, P. and Bellisio, J. A., "Ultraviolet Absorption Cross Sections for the Thallium Halide and Silver Halide Vapors," J. Chem. Phys., 50 (1969), 3563.

Drummond, D. and Schlie, L. A., "The Thallium Mercury Excimer and its Potential as a Laser," J. Chem. Phys., 65 (1976), 3454-59.

Ehrlich, D. J., Maya, J. and Osgood, R. M. Jr., "Efficient Thallium Photodissociation Laser," Appl. Phys. Lett., 33 (1978), 931-33.

Fitzsimmons, W. A., Atomic Physics, ed. by S. J. Smith, G. K. Walters (Plenum Press, New York 1973) p. 477.

Gallagher, Alan and Lurio, Allen, "Thallium Oscillator Strengths and 6d D3/2 State hfs," Phys. Rev., 136 (1964), A87-106.

Gedeon, A., Edelstein, S. A., and Davidovits, P., "Cross Sections for the Collision of Thallium (6 P1/2 and 6 P3/2) with I ," J. Chem. Phys., 55 (1974), 5171.

Hamil, R. A. et al., "Preionized Thallium-Mercury Discharge," J. Appl. Phys., 50 (1979), 637-644.

Hedges, R. E. M., Drummond, D. L., and Gallagher, A., Phys. Rev., A6 (1972), 1519.

Houterman's, F. G., Helv. Phys. Acta., 33 (1960), 933.

Kawasaki, M., Litvak, H., and Bershon, R., "Molecular Beam Photodissociation of TlI: Bond Energy and State Symmetry," J. Chem Phys., 66 (1977), 1434-36.

Komine , H. and Byer, R. L., "Optically Pumped Atomic Mercury Photodissociation Laser," J. Appl. Phys., 48 (1977), 2505-08.

Ludewigt, K., Shahdin, S., and Wellegehausen, B., "Atomic Thallium Laser and Tl-Hg Excimer Formation by Two Photon Dissociation of TlI and Hg Mixtures," Opt. Comm., 42 (1982), 143-47.

Maya, Jokab, "Quantum Efficiency of Fluorescence Excited by Photodissociation in Metal Halide Vapors and Appliciations," IEEE J. Quan. Elecs., QE-15 (1979), 579-93.

Nesmeyanov, Vapor Pressure of the Chemical Elements (Elsevier Pub. Com., London 1963) pp. 209-14, 241.

Rhodes, Ch. K., "Excimer Lasers," Topics in Applied Physics, Vol. 30 (Springer Verlag, New York 1984).

Rolsten, Robert F., Iodide Metals and Metal Iodides (Wiley, 1961) p. 267, 268.

Schlie, L. A., et al., "Strong Tl-Xe Excimer Band Emission via Electron Beam Initiated Discharges in TlI and Xe mixtures," J. Chem. Phys., 72 (1980), 4530-47.

Shahdin, S., Ludewigt, K., and Wellegehausen, B., "Photodissociative Generation of Population Inversion in Alkali Noble Gas Excimer Systems," IEEE J. Quan. Elecs., QE-17 (1981), 276-80.

Van Neen, N. JA., et al., "Photofragmentation of Thallium Halides," Chem. Phys., 55 (1981), 371-84.

Wait, John, "A Beginner's Manual for the DARE P Continuous-System Simulation Language'" CRSL Memo 311, (1978).